Functional Specialization and Flexibility in Human Association Cortex

B. T. Thomas Yeo[1,4,2,3,5], Fenna M. Krienen[5,7], Simon B. Eickhoff[8,9], Siti N. Yaakub[4], Peter T. Fox[10,11,12], Randy L. Buckner[5,7,6], Christopher L. Asplund[4,2,13] and Michael W.L. Chee[4]

[1]Department of Electrical and Computer Engineering, [2]Singapore Institute of Neurotechnology and [3]Clinical Imaging Research Centre, National University of Singapore, Singapore, [4]Center for Cognitive Neuroscience, Duke-NUS Graduate Medical School, Singapore, [5]Athinoula A. Martinos Center for Biomedical Imaging and [6]Department of Psychiatry, Massachusetts General Hospital, Boston, MA, USA, [7]Department of Psychology and Center for Brain Science, Harvard University, Cambridge, MA, USA, [8]Institute for Clinical Neuroscience and Medical Psychology, Heinrich-Heine University Düsseldorf, Düsseldorf, Germany, [9]Institute for Neuroscience and Medicine (INM-1), Research Center Jülich, Jülich, Germany, [10]Research Imaging Institute, University of Texas Health Science Center at San Antonio, San Antonio, TX, USA, [11]South Texas Veterans Health Care System, San Antonio, TX, USA, [12]State Key Laboratory for Brain and Cognitive Sciences, University of Hong Kong, Pokfulam, Hong Kong and [13]Division of Social Sciences, Yale-NUS College, Singapore

Address correspondence to B. T. Thomas Yeo, Department of Electrical and Computer Engineering, National University of Singapore, Block E4 Level 5 Room 45, 4 Engineering Drive 3, Singapore 117583. Email: thomas.yeo@nus.edu.sg

The association cortex supports cognitive functions enabling flexible behavior. Here, we explored the organization of human association cortex by mathematically formalizing the notion that a behavioral task engages multiple cognitive components, which are in turn supported by multiple overlapping brain regions. Application of the model to a large data set of neuroimaging experiments ($N = 10\,449$) identified complex zones of frontal and parietal regions that ranged from being highly specialized to highly flexible. The network organization of the specialized and flexible regions was explored with an independent resting-state fMRI data set ($N = 1000$). Cortical regions specialized for the same components were strongly coupled, suggesting that components function as partially isolated networks. Functionally flexible regions participated in multiple components to different degrees. This heterogeneous selectivity was predicted by the connectivity between flexible and specialized regions. Functionally flexible regions might support binding or integrating specialized brain networks that, in turn, contribute to the ability to execute multiple and varied tasks.

Keywords: cognitive ontology, functional connectivity, meta-analysis, parietal cortex, prefrontal cortex

Introduction

The association cortex is critical for higher cognitive functions that form the basis for flexible, adaptive behavior. Yet, clarity regarding the distribution and degree of functional specialization and domain generality within the association cortex remains elusive. We approached this conundrum with a novel strategy to mathematically model task-based neuroimaging data in relation to cognitive components engaged by the tasks. By applying the model to a large data set, insights into the functional organization of association cortex emerged.

While functional specialization is established for early sensory regions, there is uncertainty regarding the ontology of cognitive functions, how regions of association cortex support these functions, and how they relate to task paradigms commonly used in cognitive neuroscience. There are at least two reasons for this lack of consensus. First, generalizing from individual studies that infer function from a limited number of behavioral tasks can be difficult (Fox and Lancaster 2002; Wager et al. 2007). Second, it remains challenging to decompose complex behavior into meaningful neurocognitive components (Bechtel 2002; Price and Friston 2005; Poldrack 2006). For example, dorsolateral prefrontal cortex (DLPFC) is recruited by a wide range of tasks (D'Esposito et al. 1995; Miller and Cohen 2001; Petrides 2005; Badre and D'Esposito 2009; Duncan 2013), but it is unclear whether DLPFC is involved in the same cognitive process across tasks or different processes in different tasks and whether the complexity emerges because of functional diversity across subregions of DLPFC.

Meta-analysis can be a valuable means of augmenting the results of individual studies. In their influential meta-analysis, Duncan and Owen (2000) suggested that substantial portions of human prefrontal cortex (PFC) are recruited across multiple "cognitive demands" but left open the question of functional specialization. One complication of neuroimaging meta-analyses of functional specialization is that they often categorize task contrasts into distinct, non-overlapping categories a priori (but see exceptions Poldrack et al. 2012; Varoquaux et al. 2013). For example, "Anti-Saccade" and "Stroop" tasks have been used to study "response conflict" and might thus be grouped together (Duncan and Owen 2000). While carefully selected control conditions serve to isolate processes of interest, differences in the underlying composition of processes could remain. In this example, "Anti-Saccade" and "Stroop" could differ in terms of stimulus and response modalities, number of response options and response prepotency. These differences might not be completely eliminated by standard contrasts.

Dividing tasks into non-overlapping categories precludes the possibility that tasks from distinct categories might recruit common processes and tasks from the same category might recruit additional distinct processes (Fig. 1). Therefore, a brain region specialized for process "A" might be mistaken as functionally flexible if task contrasts from distinct categories recruit process "A." Conversely, a brain region flexible for processes "A" and "B" could be mistaken as functionally specific if task contrasts from the same category recruit either process "A" or "B" (in addition to processes shared across tasks within the category).

Here, we extend previous meta-analyses (e.g., Duncan and Owen 2000; Gilbert et al. 2006; Cieslik et al. 2013) by applying a novel data-driven approach to 10 449 experimental contrasts from the BrainMap® (Fox and Lancaster 2002) database. Building on the premise (Fig. 1) that different behaviors may recruit
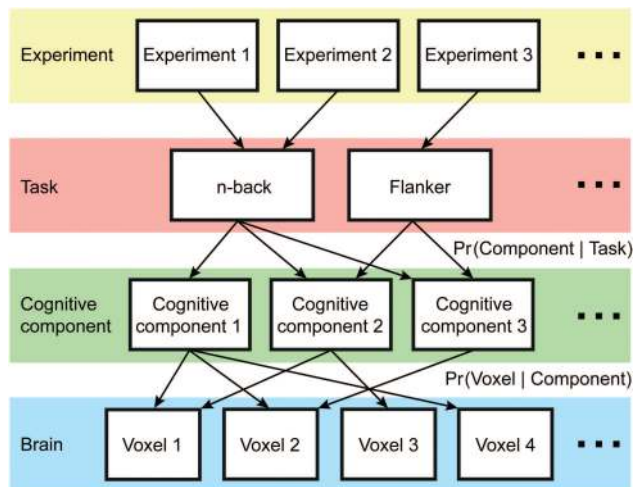
Figure 1. Relationships among experiments, tasks, cognitive components, and brain regions. Underpinning our approach is the premise that performing any given task often engages not one but several cognitive components that are in turn supported by multiple brain regions (Walton and Paul 1901; Posner et al. 1988; Mesulam 1990; Poldrack 2006). Different tasks might engage common and distinct cognitive components. Furthermore, different components may activate common and distinct brain regions. Here, we demonstrated that the framework can be instantiated with a formal mathematical model (Rosen-Zvi et al. 2010), whose parameters can be estimated. The estimated model parameters are the probability that a task would recruit a cognitive component for an activation focus (i.e., Pr(component | task)) and the probability a cognitive component would activate a brain voxel for an activation focus (i.e., Pr(voxel | component)). The model parameters enabled us to derive quantitative maps of functional specialization and flexibility across the cerebral cortex. Here, the term "cognitive component" is operationally defined as latent variables within the mathematical model (Supplementary Fig. 1).

distinct and overlapping sets of brain regions (Walton and Paul 1901; Posner et al. 1988; Mesulam 1990; Price and Friston 2005; Poldrack 2006), our approach allowed us to consider principles of functional organization not easily captured by prior meta-analyses. More specifically, we developed a formal mathematical instantiation of Figure 1, whose model parameters can be estimated from the meta-analysis. This allowed the identification of cognitive components that are shared across tasks, without pre-defining task membership. The estimated parameters enabled the derivation of quantitative maps of functional specialization and flexibility across the cerebral cortex. The network organization of these functionally specific and flexible regions was further characterized using an independent resting-state fMRI data set (N = 1000).

The results advance our understanding of association cortex organization in several ways. First, we identified a set of cognitive components, each of which was associated with meaningful distributions of tasks and brain activations. Second, there were numerous association regions that were functionally specific for distinct cognitive components. Regions specialized for the same cognitive components were strongly coupled during the resting state, suggesting that components are supported by partially isolated networks. Although there have been many prior studies demonstrating functional specificity, there are ongoing debates regarding the nature of the specializations (e.g., Mitchell 2008; Young et al. 2010). Without careful experimental manipulations, we do not suggest that meta-analysis will fully resolve these issues. Nevertheless, by aggregating evidence across thousands of experiments, our meta-analysis provides a consensus map of functional specialization and flexibility in the human cerebral cortex. Third, we confirmed

the presence of functionally flexible regions in frontal and parietal cortex that participated in multiple components (Fedorenko et al. 2013). Moreover, the functionally flexible regions were themselves heterogeneous, that is, while the regions support multiple cognitive components, each does so to a *different* degree. The resting-state connectivity of the flexible regions predicted their selectivity to specialized regions of different components. One possibility is that functionally flexible regions integrate information from segregated brain networks specialized for distinct functions.

Methods

Overview

A hierarchical Bayesian model (Fig. 1) was applied to 10 449 experimental contrasts in the BrainMap database to obtain cognitive components shared across 83 BrainMap-defined task categories. The model captures the premise that behavioral tasks recruit multiple overlapping cognitive components, which are in turn supported by overlapping brain regions. Subsequent analyses proceeded in four stages. First, the estimated components were examined for insights into tasks involving motor processing or cognitive control. Next, we explored how the estimated components changed as a function of the number of components. The estimated model parameters were then utilized to compute maps of functional specificity and flexibility across the cerebral cortex, focusing on lateral frontal and parietal cortices. Finally, an independent resting-state fMRI data set (N = 1000) was employed to explore the network organization of the functionally specific and flexible regions.

BrainMap

At the time of analysis, the BrainMap database (Fox and Lancaster 2002) contained findings from 2194 journal articles. Each study typically comprised multiple experiments, defined by BrainMap as the comparison of 2 or more imaging conditions resulting in an activation image. For example, a study employing the "n-back" task might include an experimental contrast comparing "3-back" with "0-back" and another comparing "3-back" with "1-back," resulting in 2 activation maps. The 2194 studies were associated with 10 449 experimental contrasts and 83 178 activation foci.

The spatial locations of these activations were represented via the coordinates of statistically significant local maxima in the activation images. All foci coordinates were in or transformed to the MNI152 coordinate system (Lancaster et al. 2007). Following standard analysis procedure (Wager et al. 2007; Yarkoni et al. 2011), a 2-mm-resolution binary activation image was constructed for each experimental contrast, where a voxel was assigned a value of 1 if it was within 10 mm of any activation focus and 0 otherwise.

In BrainMap, each experiment is tagged with 1 or more task categories. At the time of analyses, there were 83 task categories (e.g., "n-back" and "Flanker"), referred to as "paradigm classes" in the BrainMap lexicon. Definitions of the 83 tasks can be downloaded here 〈https://surfer.nmr.mgh.harvard.edu/fswiki/BrainmapOntology_Yeo2015〉. The definitions of the task categories were driven by common usage in the literature and were often stated explicitly in the papers (Fox et al. 2005). Therefore, they provide a relatively objective (albeit imperfect) means for organizing the 10 449 experiments while preserving considerable depth of content, as indicated by the 83 unique identifiers.

Author-Topic Hierarchical Bayesian Model

We sought a mathematical model that captured the premise that performing a task results in the recruitment of multiple cognitive components supported by multiple brain regions (Fig. 1). Furthermore, the model should allow for the possibility that tasks recruit overlapping components and brain regions participate in multiple components. Among the many (unlimited) models satisfying the above-mentioned requirements, the author-topic model (Supplementary Fig. 1) was perhaps the simplest and was therefore applied to the BrainMap database.

The author-topic model was originally developed for analyzing text corpora (Rosen-Zvi et al. 2010). The model assumes that a text document is composed of an unordered collection of words written by a group of authors. Each author is represented by a probability distribution over (hidden) topics, and each topic is represented by a probability distribution over a dictionary of words. Given a collection of text documents, there exist algorithms to estimate the distribution of topics associated with each author and the distribution of dictionary words associated with each topic (Rosen-Zvi et al. 2010). The author-topic model is useful because it allows for the identification of a document to be composed of multiple topics (which can be shared across documents), and each topic can be composed of multiple words (which can be shared across topics).

To map the author-topic model to Figure 1, one can think of experimental contrasts (instead of text documents), BrainMap task categories (instead of authors), cognitive components (instead of topics), MNI152 voxels (instead of dictionary words) and activation foci (instead of document words). Here, "cognitive components" refers to the latent variables within the mathematical model (Supplementary Fig. 1), bridging between tasks and brain activation. The term "cognitive" is used broadly to encompass components (e.g., motor and affective) that may not be typically considered cognitive.

Under the author-topic model, suppose there are F activation foci reported in an experiment utilizing a set of tasks (in most cases, the set of tasks consists of a single-task category (e.g., n-back). A small percentage of experiments in BrainMap utilized tasks from >1 task category). The fth activation focus is assumed to be generated by first randomly selecting a task from the set of tasks associated with the experiment. Given the task, a component is then randomly selected based on the probability that the task would recruit a component (Pr(component | task)). Given the component, the voxel location of the activation focus is then randomly selected based on the probability that the component would activate a voxel (Pr(voxel | component)). We denote the entire collection of Pr(component | task) and Pr(voxel | component) as θ and β, respectively. Therefore, θ and β are matrices, where each row is a categorical distribution summing to 1. For example, the 11th row and 14th column of θ corresponds to Pr(14th component | 11th task) and the 20th row and 50th column of β corresponds to Pr(50th voxel | 20th component).

The author-topic model assumes that the ordering of words within a document is exchangeable. In the context of our application, the corresponding assumption is that the ordering of activation foci is exchangeable. Although word order in real documents is important, the ordering of foci (e.g., prefrontal vs. parietal) reported in an experiment is arbitrary and thus consistent with the assumption. Consequently, the author-topic model appears particularly well-suited for application to the present context.

Given the 10 449 BrainMap experiments with associated activation coordinates and task categories, as well as the number of cognitive components N_C, the probabilities θ and β were estimated using Gibbs sampling (Rosen-Zvi et al. 2010) and expectation maximization (Dempster et al. 1977). Further mathematical and implementation details are found in Supplementary Material.

Interpreting the Model Parameters
Since Pr(component | task) summed to 1 over all components, one might be concerned that greater recruitment of 1 component might reduce recruitment of other components. However, the probabilities should be interpreted within the context of the model from which the probabilities were estimated. Under the author-topic model, Pr(component | task) should be strictly interpreted as the probability of a task recruiting a cognitive component *for an activation focus* and not the probability of a task recruiting a component *for an entire experiment*. For example, suppose there were 5 activation foci for an experiment using task T and Pr(component X | Task T) was only 0.3. Then, the probability that task T recruits component X *for the entire experiment* is equal to the probability that component X was recruited for at least 1 focus, that is, $1 - (1 - 0.3)^5 = 0.83$.

A task recruiting more components would have lower Pr(component | task) on average because the probability sums to 1 over all components. However, the task might also result in more activation foci on average. For instance, a theory of mind task requiring visual imagery might (on average) report more activation foci than a visual imagery task alone, because the theory of mind task with visual imagery would have activation foci associated with both theory of mind and visual processing.

Considering the above, Pr(voxel | component) should be strictly interpreted as the probability of a voxel activated by a cognitive component *for an activation focus*. Nevertheless, as will be seen, control analyses including those utilizing a separate resting-state data set suggested that Pr(component | task) and Pr(voxel | component) summing to 1 was not a serious confound.

An alternative (but not necessarily more biologically plausible) model, where Pr(voxel | component) and Pr(component | task) do not sum to 1 over all voxels and components, respectively, is discussed in Supplementary Material. Such a model is currently computationally infeasible.

Displaying Pr(component | task) and Pr(voxel | component)
The Circos software (Krzywinski et al. 2009) was used to visualize the full matrix Pr(component | task), θ (Fig. 2). For visualization purposes, tasks with similar Pr(component | task) were more closely positioned. More specifically, Pr(component | task) was clustered with the linkage algorithm (Matlab 7.11: "average" method, "correlation" metric) and the resulting dendrogram was used to order the tasks. This visualization strategy was especially useful for interactive exploration of the estimated ontology: https://surfer.nmr.mgh.harvard.edu/fswiki/BrainmapOntology_Yeo2015, last accessed September 12, 2014.

Pr(component | task) was also plotted as a colored matrix (Fig. 3). Given space constraints, only a reduced set of tasks meeting 2 selection criteria are shown. The first selection criterion was that the tasks were among the top 5 tasks for at least 1 component. The second criterion was that the task was utilized by at least 10 unique studies. Because certain tasks were among the top 5 tasks of >1 components, the reduced task set for the 12-component estimate contained 51 tasks (instead of 60). The ordering of the tasks was the same as the Circos visualization.

The matrix Pr(voxel | component), β, can be interpreted as N_C brain images in MNI152 space. Volumetric slices highlighting certain subcortical structures were displayed using FreeSurfer (Fischl 2012). To visualize the cerebral cortex, the volumetric images were transformed to PALS-B12 surface space using Caret (Van Essen and Dierker 2007) via the FreeSurfer surface space (Fischl 2012). The details of these transformations have been previously described (Buckner et al. 2011; Yeo et al. 2011).

For visualization, Pr(component | task) was thresholded at $1/N_C$, whereas Pr(voxel | component) was thresholded at $1e-5$. Given that there were 284 100 voxels within the MNI152 brain mask, thresholding Pr(voxel | component) at $1e-5$ ($\approx 3 \times 1/284\,100$) is relatively stringent. There is no simple way of thresholding the model estimates. Consequently, the unthresholded model estimates for 10 to 14 components are made publicly available (https://surfer.nmr.mgh.harvard.edu/fswiki/BrainmapOntology_Yeo2015, last accessed September 12, 2014). To allow easier interpretation, only task categories with at least 10 unique studies were considered in the creation of tables and figures emphasizing the top task categories for each component.

Number of Cognitive Components
An important model parameter is the number of cognitive components. Therefore, how the estimated components changed as a function of the number of components was explored in two ways. First, cross-validation was utilized to evaluate the model generalization power as a function of the number of cognitive components N_C. More specifically, the model parameters were estimated based on a random 95% subset of the data, and the resulting generalization power was computed on the remaining 5% of the data. Generalization power was defined as the negative of the perplexity measure (Section 7.1 of Blei et al. 2003), so larger values corresponded to strong generalization power. This procedure was repeated 100 times and the generalization power was averaged, resulting in a plot

of averaged generalization power as the number of cognitive components was increased from 2 to 20.

Second, an exhaustive search was employed to assess the possibility that 2 unknown components of the $(N+1)$-component estimate were subdivisions of an unknown component of the N-component estimate (while the remaining $N-1$ components were consistent across both estimates). This exhaustive search yielded a hypothesized subdivision with associated correlation values quantifying the quality of the subdivision. The procedure was repeated from $N=2$ to $N=19$. The correlation values were plotted as a function of N. High correlation values implied evidence for a nested ontology. Details of the exhaustive search are found in Supplementary Material.

To foreshadow the results, from 6 to 16 components, the components were found to divide into subcomponents as the number of components increased, revealing a nested ontology. The nested ontology suggested that the estimates derived from the different number of cognitive components might provide distinct insights. Because the 12-component estimate provided additional insights into cognitive control tasks (see Results), the remaining analyses were performed using the 12-component estimate.

Functional Flexibility

Although the cognitive components were estimated in (MNI152) volumetric space, the estimation quality was significantly better in the cerebral cortex compared with subcortical structures, likely because of the relatively large size of the former and inconsistent reporting of the latter. For example, full coverage of the cerebellum is not always achieved by typical slice prescriptions. Consequently, the subsequent analyses will focus on the cerebral cortex.

To quantify the functional flexibility of cortical regions under the 12-component estimate, for each voxel, the number of components with Pr(voxel | component) at least 1e − 5 was computed (Fig. 6). As previously discussed, 1e − 5 is a relatively stringent threshold. Since there is no simple way of determining a threshold, different thresholds were explored and qualitatively similar results (not shown) were obtained.

The functional flexibility estimate was compared with an estimate of the multiple-demand (MD) system (Fedorenko et al. 2013; http://imaging.mrc-cbu.cam.ac.uk/imaging/MDsystem, last accessed September 12, 2014). Both estimates were mapped to the FreeSurfer surface space. The resulting surface maps were compared by computing the Pearson's correlation between them.

Functional Specificity

To explore functional specialization within the cerebral cortex, the 12-component estimate of Pr(voxel | component) was mapped onto the FreeSurfer surface space, resulting in estimates of the probability that a component would activate each surface vertex, Pr(vertex | component). Nearest neighbor smoothing (1 iteration) of Pr(vertex | component) was performed, and Bayes' rule was used to compute Pr(component | vertex):

$$\text{Pr}(component \mid vertex) \propto \text{Pr}(vertex \mid component)\,\text{Pr}(component)$$

Given that there is no a priori reason to assume some cognitive components are more common than others, Pr(component) was set to be $1/N_C$. For a given vertex, the ranking of components was therefore the same for Pr(component | vertex) and Pr(vertex | component). Pr(component | vertex) can be interpreted as follows: Given an activation focus was located at a vertex, Pr(component | vertex) is the probability that a particular cognitive component was recruited for the activation focus.

For each vertex, the ratio between the top 2 components was computed as a quantitative measure of functional specificity:

$$\frac{\text{Pr}\,(Most\ Likely\ Component\ \text{at}\ Vertex \mid Vertex)}{\text{Pr}\,(Second\ Most\ Likely\ Component\ \text{at}\ Vertex \mid Vertex)}$$

A ratio of 2 implied that for a given activated vertex, the top component would be twice as likely to be recruited as the second most likely

component. A functional specificity of 2 was interpreted as having a certain degree of functional specialization.

For example, consider a vertex with Pr(C1 | vertex) = Pr(C4 | vertex) = Pr(C5 | vertex) = 0.1, Pr(C2 | vertex) = 0.2 and Pr(C3 | vertex) = 0.5. The most and second most likely components for the vertex would be C3 and C2, respectively. The vertex would have a functional specificity value of 0.5/0.2 = 2.5, indicating functional specificity.

Ultimately, any operational definition of functional flexibility or specificity overlooks certain complexities of the model estimates since 12 numbers per voxel (or vertex) are reduced to a single number. Our model estimates have been made publicly available, allowing other researchers to explore different specificity and flexibility criteria with the given estimates.

Statistical Significance of Functional Specificity

The functional specificity measure was computed across the entire cerebral cortex. To compute the statistical significance, a null distribution of functional specificity was generated using a Monte-Carlo simulation approach similar to that used in standard meta-analyses (Wager et al. 2007; Eickhoff et al. 2012). Briefly, a set of 10 449 random experiments was simulated by generating foci coordinates based on the spatial distribution of foci in the BrainMap database. The spatial distribution of BrainMap foci was used to generate the null distribution, addressing the non-uniform spatial distribution of foci in the literature (Poldrack 2011; Behrens et al. 2013; Langer et al. 2014).

The number of foci was matched between corresponding pairs of real and random experiments. Pr(voxel | component) and corresponding functional specificity were then estimated based on this simulated set of 10 449 experiments. Each simulated data set allowed the generation of 299 881 null functional specificity values (corresponding to the resolution of FreeSurfer surface space). This procedure was repeated 100 times to generate a complete null histogram, which was then used to assign P-values to the original functional specificity values. False discovery rate was set at $q < 0.05$, correcting for multiple comparisons across all vertices representing the cerebral cortex. For visualization purpose, functionally specialized regions with <20 vertices were removed. Results were transformed and visualized in PALS-B12 surface space (Van Essen and Dierker 2007).

Alternative Analysis of Functional Specificity

The author-topic model encodes the premise that performing a task recruits multiple cognitive components supported by multiple brain regions. However, there are multiple mathematical models consistent with the premise, that is, the choice of model is not unique. To ensure the functional specificity estimates were robust to the particular model and estimation procedure, the data were re-analyzed using a simple procedure that categorized tasks into distinct groups, simulating traditional meta-analyses (Duncan and Owen 2000; Shackman et al. 2011).

For each BrainMap task category (with at least 10 unique studies), the probability that a task category would activate a particular brain location Pr(voxel | task) was computed by averaging the binary activation images of experiments utilizing only that task category. Contrary to the author-topic model estimates, Pr(voxel | task) is not a probability distribution over voxels and does not sum to 1 over all voxels. Instead, Pr(voxel | task) is the probability that a voxel is activated in an experiment utilizing only that task (rather than the probability that a task would activate a voxel *for an activation focus*). The Pr(voxel | task) was transformed onto the FreeSurfer surface space, resulting in estimates of the probability that a task would activate different surface mesh vertices Pr(vertex | task). The Pr(vertex | task) was averaged across the top K tasks of each cognitive component, resulting in an average probability that the top K tasks of each component would activate a vertex Pr(vertex | top K tasks).

To foreshadow the results, the functional specificity estimates (previous section) revealed islands of specificity in lateral frontal and parietal cortex. For this alternative functional specificity analysis, the islands were extracted as regions of interest (ROIs) resulting in 41 ROIs. Since the value of K was arbitrary, we considered K from 1 to 10. For each ROI and each component, Pr(vertex | top K tasks) was averaged across the vertices of the ROI. Therefore, for each ROI, it was

determined whether the component with the highest average Pr (vertex | top K tasks) was also the mostly likely component according to the author-topic model.

Resting-State fMRI Data Set

Neuroimaging tasks may reflect an incomplete corpus of cognitive processes, and the representation of functional domains is not uniform. There may also be possible biases due to the non-uniform distribution of activation foci (Poldrack 2011; Behrens et al. 2013). Consequently, an independent resting-state fMRI data set was employed to test the findings from the functional specificity analysis. The data set consists of 1000 subjects between ages 18 and 35 (mean age = 21.3; 42.7% male) who underwent 1 or 2 runs of passive eyes open rest scans. Analyses of the data set have been published previously (Buckner et al. 2011; Yeo et al. 2011; Choi et al. 2012).

Data were acquired on 3 T Tim Trio scanners (Siemens, Erlangen, Germany) using a 12-channel phased-array head coil. Functional data consisted of gradient-echo echo-planar images (EPIs) sensitive to blood oxygenation level-dependent contrast. The EPI parameters were as follows: repetition time = 3000 ms, echo time = 30 ms, flip angle = 85°, $3 \times 3 \times 3$ mm voxels, field of view = 216, and 47 axial slices collected with interleaved acquisition. Slices were oriented along the AC–PC plane. Functional runs lasted 6.2 min (124 time points). Structural data included a multiecho T1-weighted magnetization-prepared gradient-echo (MP-RAGE) image. More details of the acquisition can be found elsewhere (Yeo et al. 2011).

Resting-State fMRI Preprocessing

fMRI processing steps included 1) discarding the first 4 frames of each run, 2) correcting for slice acquisition-dependent time shifts in each volume with statistical parametric mapping software, and 3) correcting for head motion using rigid body translation and rotation parameters (FMRIB software library; Smith et al. 2004). This was followed by standard functional connectivity preprocessing (Yeo et al. 2011). Briefly, linear trends over each run were removed and a low-pass temporal filter retained frequencies of <0.08 Hz. Spurious variance was removed using linear regression with terms for head motion, whole brain signal, ventricle signal, white matter signal and their derivatives.

Individual participants' T1 scans were reconstructed into surface representations using FreeSurfer (Fischl 2012). Functional data were registered to structural images using FreeSurfer's FsFast package (Greve and Fischl 2009). Functional data were projected onto the FreeSurfer surface space (2-mm mesh), smoothed on the surface using a 6-mm full-width half-maximum kernel, and down-sampled to a 4-mm mesh.

Functional Connectivity of Functionally Specific Regions

Each functionally specific island in the cerebral cortex was extracted as an ROI. The functional connectivity between 2 ROIs was defined as the Pearson's correlation between the averaged fMRI time courses of the ROIs. The correlation was computed for individual subjects and converted into z-values using the Fisher's r-to-z transformation before averaging across pairs of ROIs. Two-tailed, paired-sample t-tests (df = 999) tested the hypothesis that cortical regions specialized for the same cognitive components were more strongly coupled than regions with different specializations.

Functional Connectivity of Functionally Flexible Regions

A surprising result (see Results) was that many functionally flexible regions were selective for different cognitive components. The possibility that functional heterogeneity across functionally flexible regions might relate to distinct connectivity patterns (Goldman-Rakic 1988; Passingham et al. 2002; Saygin et al. 2012) was further explored.

Cortical vertices with at least 1e − 5 probability of being activated by 2 components (i.e., same criterion as the "Functional Flexibility" section) were considered. For each functionally flexible vertex and for each subject, the Pearson's correlation (functional connectivity) was computed between the vertex's time course and the averaged fMRI time courses of each functionally specialized ROI defined in the previous

section. If the functionally flexible vertex overlapped with a functionally specific ROI, the ROI was excluded from the analysis (our operational definitions of flexibility and specificity are not opposite measures. A flexible region is activated by multiple components with high probability, whereas a specific region is preferentially activated by 1 component relative to other components. Therefore, flexibility and specificity are not mutually exclusive by definition. Indeed, there were some regions that had both a high likelihood of being activated by multiple components (functionally flexible) and a much higher likelihood of being activated by a given component than other components (functionally specific). Such occurrences were rare and were generally located near the borders of specific and flexible zones). The functional connectivity values were converted into z-values using the Fisher's r-to-z transformation before averaging across ROIs specialized for the same component. This resulted in 12 averaged functional connectivity values for *each* vertex and *each* subject.

To obtain an overall map of correlation between selectivity (Pr(component | functionally flexible vertex)) and functional connectivity, the 12 functional connectivity values for each functionally flexible vertex were averaged across the 1000 subjects and then correlated with Pr (component | vertex). These correlations were averaged across all functionally flexible vertices to provide an overall correlation.

Finally, to formally test the hypothesis that functional heterogeneity across functionally flexible regions might arise from distinct connectivity patterns, the 12 functional connectivity values for each functionally flexible vertex were correlated with its selectivity (Pr(component | vertex)) *without* averaging across subjects. These correlations were then averaged across all functionally flexible vertices, and a two-tailed, one-sample t-test (df = 999) was performed.

Results

Overview

The hierarchical Bayesian model (Fig. 1 and Supplementary Fig. 1) was applied to the BrainMap database (10 449 experimental contrasts) to obtain cognitive components shared across 83 BrainMap-defined task categories. The utility of this approach was demonstrated by showing how different motor and cognitive control tasks recruited overlapping cognitive components, and how these components comprised of overlapping brain regions.

An important parameter in the model is the number of cognitive components. Therefore, we explored how the estimated components changed as a function of the number of components. As the number of components increased, the components divided into subcomponents, revealing a nested ontology.

The estimated model parameters were used to compute maps of functional specificity and flexibility across the cerebral cortex. An independent resting-state fMRI analysis (N = 1000) revealed that cortical regions specialized for the same cognitive components were more strongly coupled than those with different specializations. Furthermore, functionally flexible regions possess connectivity patterns consistent with their selectivity for different cognitive components.

12-Component Ontology

The hierarchical Bayesian model (Fig. 1 and Supplementary Fig. 1) allowed estimation of the probability that each task would recruit different cognitive components (i.e., Pr(component | task)) and the probability that each component would activate different voxels (i.e., Pr(voxel | component)). Here, we focus on 12 cognitive components (see "Nested Ontology" for justification).

The 83 BrainMap-defined tasks recruited overlapping cognitive components to varying degrees (Figs. 2a and 3). For ease of visualization, tasks with similar Pr(component | task) were
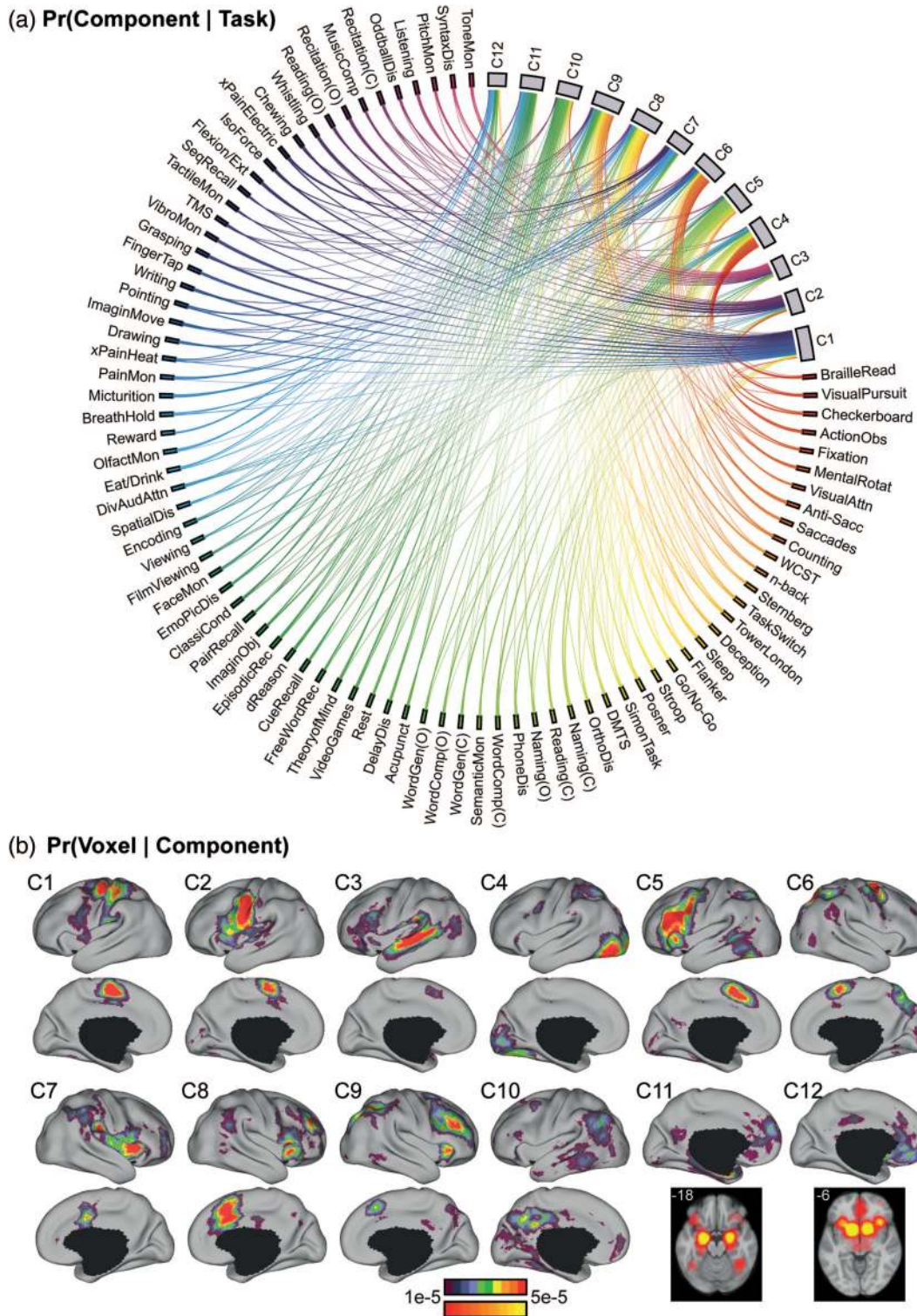
Figure 2. 12-component model estimates. (*a*) Probability of tasks recruiting different components (i.e., Pr(component | task)). The components, C1 to C12, lie on the top right. The 83 tasks lie in the remaining segments of the circle. Each line connects 1 task with 1 cognitive component. The thickness of the lines is proportional to the magnitude of Pr (component | task). For the purpose of visualization, tasks with similar Pr(component | task) are more closely positioned and their lines were assigned similar colors. Only lines corresponding to Pr(component | task) > 1/12 are shown. (*b*) Probability of components activating different brain voxels (i.e., Pr(voxel | component)). The cerebral hemisphere with the stronger activation is shown, although most components have high probabilities of bilateral activation. An exception is component C5, which has high probability of activating the left, but not the right, cerebral cortex. Many components, especially C11 and C12, activate subcortical regions. Component C7 had high probability of activating the brainstem (Supplementary Fig. 2). The top color bar is utilized for the surface-based visualization of Pr(voxel | component), whereas the bottom color bar is utilized for the volumetric slices highlighting subcortical structures shown for components C11 and C12. Additional slices highlighting subcortical structures are found in Supplementary Figure 2. (C) indicates "covert" and (O) indicates "overt". An interactive version of the model estimates and the unthresholded estimates for 10-component to 14-component estimates are available: https://surfer.nmr.mgh.harvard.edu/fswiki/BrainmapOntology_Yeo2015, last accessed September 12, 2014.

placed adjacent to one another (see Methods). Several cognitive components (e.g., C1) were heavily recruited by adjacent tasks. However, there were also components (e.g., C4) recruited by dispersed clusters of tasks. Therefore, our model allows for different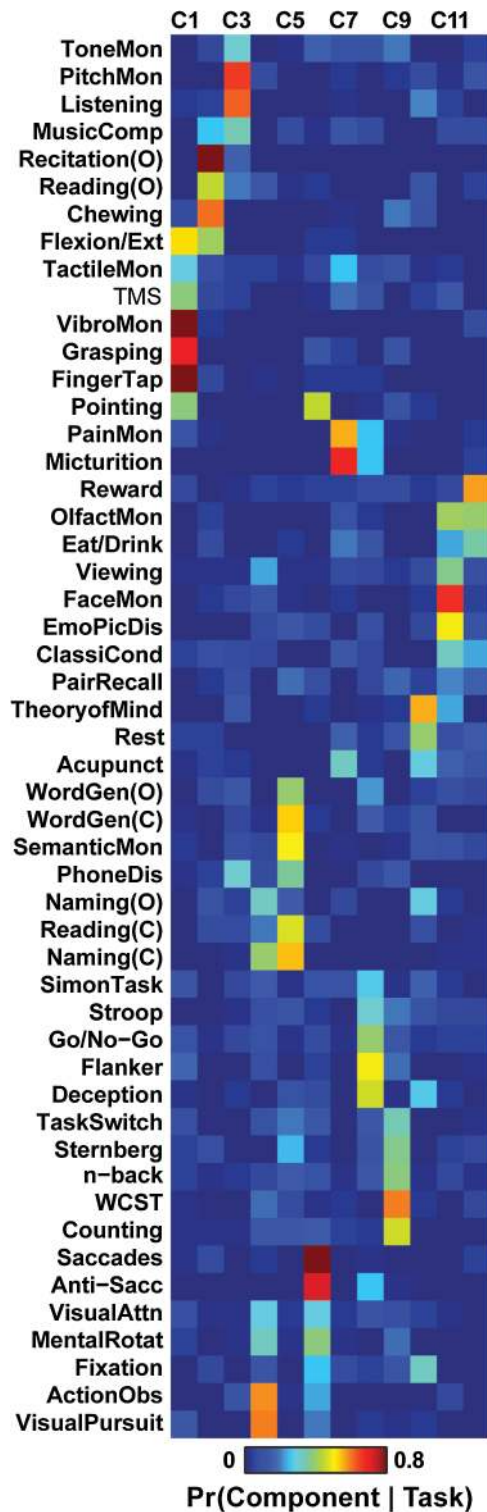 tasks to recruit common and distinct cognitive components. The resulting representation extends models that classify tasks into distinct, non-overlapping groups (e.g., Laird et al. 2011).

Just as different tasks recruited overlapping cognitive components, different components activated common and distinct brain regions to varying degrees (Fig. 2b and Supplementary Fig. 2). Each component activated a distributed, but distinct pattern of brain voxels, spanning multiple cortical lobes (Fig. 2b) and subcortical structures (Supplementary Fig. 2). No component appears particularly diffuse (Supplementary Fig. 3). Therefore, our approach extends models that assume each brain region belongs to a single category or cluster (e.g., Cieslik et al. 2013; Clos et al. 2013).

A publicly available version of Figure 2 can be used to interactively explore the ontology: https://surfer.nmr.mgh.harvard.edu/fswiki/BrainmapOntology_Yeo2015, last accessed September 12, 2014. The Pr(component | task) of the top 5 tasks for each component are shown in Table 1. We will now briefly discuss each component.

Component C1 had high probability of activating regions at or near the supplementary motor area (Fig. 2b), the hand representation in the somato-motor cortex and the hand representation in the cerebellum (Supplementary Fig. 2a). The top tasks recruiting C1 were "Vibrotactile Monitoring/Discrimination," "Finger Tapping," and "Grasping."

Figure 3. Alternative visualization of the probability of tasks recruiting different components Pr(component | task). For the purpose of visualization, tasks with similar Pr(component | task) are more closely positioned. Due to space constraints, only 51 tasks are shown (see Methods). (C) = Covert; (O) =Overt.

Table 1:
Top five tasks recruiting 12 components

Pr(C1 | task)		Pr(C2 | task)	
Vibrotactile Mon/Discrim	0.9	Recitation/Repetition (O):	0.84
Finger Tapping	0.8	Chewing/Swallowing:	0.81
Grasping	0.71	Reading (Overt):	0.74
Flexion/Extension	0.52	Flexion/Extension:	0.47
TMS	0.39	Music Comp/Production:	0.26
Pr(C3 | task)		**Pr(C4 | task)**	
Pitch Mon/Discrim	0.66	Visual Pursuit/Tracking	0.59
Passive Listening	0.62	Action Observation	0.58
Music Comp/Production	0.33	Naming (C)	0.39
Tone Mon/Discrim	0.3	Naming (O)	0.32
Phonological Discrim	0.3	Mental Rotation	0.32
Pr(C5 | task)		**Pr(C6 | task)**	
Naming (C)	0.55	Saccades	0.8
Word Generation (C)	0.53	Anti-Saccades	0.72
Semantic Mon/Discrim	0.5	Pointing	0.44
Reading (C)	0.47	Mental Rotation	0.39
Word Generation (O)	0.39	Visual Distractor/Attn	0.28
Pr(C7 | task)		**Pr(C8 | task)**	
Micturition	0.68	Flanker	0.49
Pain Mon/Discrim	0.56	Deception	0.45
Acupuncture	0.32	Go/No-Go	0.39
Tactile Mon/Discrim	0.26	Stroop	0.31
Eating/Drinking	0.2	Simon	0.27
Pr(C9 | task)		**Pr(C10 | task)**	
WCST	0.59	Theory of Mind	0.53
Counting/Calculation	0.45	Rest	0.39
n-back	0.38	Fixation	0.32
Sternberg	0.37	Naming (O)	0.28
Task Switching	0.33	Acupuncture	0.28
Pr(C11 | task)		**Pr(C12 | task)**	
Face Mon/Discrim	0.67	Reward Task	0.57
Subj Emo Pict Discrim	0.49	Olfactory Mon/Discrim	0.39
Olfactory Mon/Discrim	0.41	Eating/Drinking	0.35
Passive Viewing	0.37	Classical Conditioning	0.23
Classical Conditioning	0.32	Paired Associate Recall	0.16

Notes: Only the top 5 tasks for each cognitive component are shown. Unthresholded and unfiltered model estimates for 10 to 14 components are publicly available: https://surfer.nmr.mgh.harvard.edu/fswiki/BrainmapOntology_Yeo2015, last accessed September 12, 2014. "(C)" and "(O)" indicate "covert" and "overt" respectively. "Mon", "Discrmin" and "Attn" are short for "monitoring", "discrimination" and "attention" respectively. "Subj Emo Pict Discrimin" is short for "Subjective Emotional Picture Discrimination".

Component C2 had high probability of activating regions at or near the supplementary motor area (Fig. 2*b*), the face representation in the somato-motor cortex and the face representation in the cerebellum (Supplementary Fig. 2*a*). The top tasks recruiting C2 were "Overt Recitation/Repetition," "Chewing/Swallowing," and "Overt Reading."

Component C3 had high probability of activating the auditory cortex, as well as the posterior medial frontal cortex and inferior frontal gyrus (IFG). The top tasks recruiting C3 were "Pitch Monitoring/Discrimination," "Passive Listening," and "Music Comprehension/Production."

Component C4 had high probability of activating the occipital lobe, as well as the inferior temporal cortex and superior parietal cortex. The top tasks recruiting component C4 were "Visual Pursuit/Tracking," "Action Observation," and "Covert Naming."

Component C5 had high probability of activating the posterior medial frontal cortex, IFG, posterior lateral frontal cortex, as well as the superior parietal cortex, temporal cortex, and cerebellum. The activation pattern was left lateralized in the cerebral cortex (Fig. 2*b*) and right lateralized in the cerebellum (Supplementary Fig. 2*a*). The top tasks recruiting component C5 were "Covert Naming," "Covert Word Generation," and "Semantic Monitoring/Discrimination."

Component C6 had high probability of activating the posterior medial frontal cortex, superior parietal cortex, and the junction of the superior frontal and precentral sulci, which is at or near the human homolog of the frontal eye fields (Koyama et al. 2004). The activations associated with C6 overlapped significantly with brain regions associated with visual spatial attention (Corbetta et al. 2008; Szczepanski et al. 2010). The top tasks recruiting component C6 were "Saccades," "Anti-Saccades," and "Pointing."

Component C7 had high probability of activating the insula, frontal operculum, parietal operculum, and the brain stem (Supplementary Fig. 2*b*). The top tasks recruiting component C7 were "Micturition," "Pain Monitoring/Discrimination," and "Acupuncture."

Component C8 had high probability of activating the anterior mid-cingulate cortex, posterior medial frontal cortex, anterior insula, anterior lateral PFC, as well as the temporoparietal junction. The top tasks recruiting component C8 were "Flanker," "Deception," and "Go/No-Go."

Component C9 had high probability of activating the superior parietal cortex, intraparietal sulcus, lateral PFC, anterior insula, and posterior medial frontal cortex. The top tasks recruiting component C9 were "Wisconsin Card Sorting Test," "Counting/Calculation," and "n-back."

Component C10 had high probability of activating the posterior cingulate cortex, precuneus, posterior hippocampal formation, medial PFC, inferior parietal cortex, temporal cortex, and the temporoparietal junction. The activations associated with C10 overlapped significantly with the default network (Buckner et al. 2008). The top tasks recruiting component C10 were "Theory of Mind," "Rest," and "Fixation."

Component C11 had high probability of activating the anterior hippocampus, amygdala (Supplementary Fig. 2*c*), as well as the posterior cingulate cortex and medial PFC. The top tasks recruiting component C11 were "Face Monitoring/Discrimination," "Subjective Emotional Picture Discrimination," and "Olfactory Monitoring/Discrimination."

Component C12 had high probability of activating the ventral striatum (Supplementary Fig. 2*d*), anterior insula, and ventral medial frontal cortex. The top tasks recruiting component C12 were "Reward Task," "Olfactory Monitoring/Discrimination," and "Eating/Drinking."

The topography of subcortical activation was generally consistent with known subcortical organization and the top tasks recruiting each component (Supplementary Fig. 2). For example, components C1, C2, and C5 activated distinct cerebellar territories from anterior to posterior (Supplementary Fig. 2*a*), consistent with known cerebellar organization (Stoodley and Schmahmann, 2009). This result provides additional details that extend previous meta-analytic approaches (Smith et al. 2009; Laird et al. 2011), which extracted the entire cerebellum as a single component. While the subcortical activation patterns increased our confidence in the component estimates, the estimation quality was significantly better in the cerebral cortex because the subcortical structures are much smaller and often neglected in functional experiments. For example, the posterior cerebellum is often omitted in fMRI data acquisition. Consequently, the functional specificity and flexibility analyses focused only on the cerebral cortex.

In describing the 12 components, we have refrained from explicitly labeling the cognitive components in order to not bias the readers' interpretation. Some labels would likely be uncontroversial. For instance, there would probably be agreement that tasks involving touch or hand movement are likely to recruit C1, which could therefore be labeled as somatosensory/motor. However, other components may have several possible interpretations. For example, the top tasks recruiting component C8 were "Flanker," "Deception," and "Go/No-Go." One interpretation is that C8 might be associated with tasks requiring inhibition of pre-potent responses (Miyake et al. 2000). However, the component can also reasonably be tagged as "response conflict" (Duncan and Owen 2000). Conventional task-based experiments, rather than meta-analyses, are more appropriate for disambiguating such differences in interpretation.
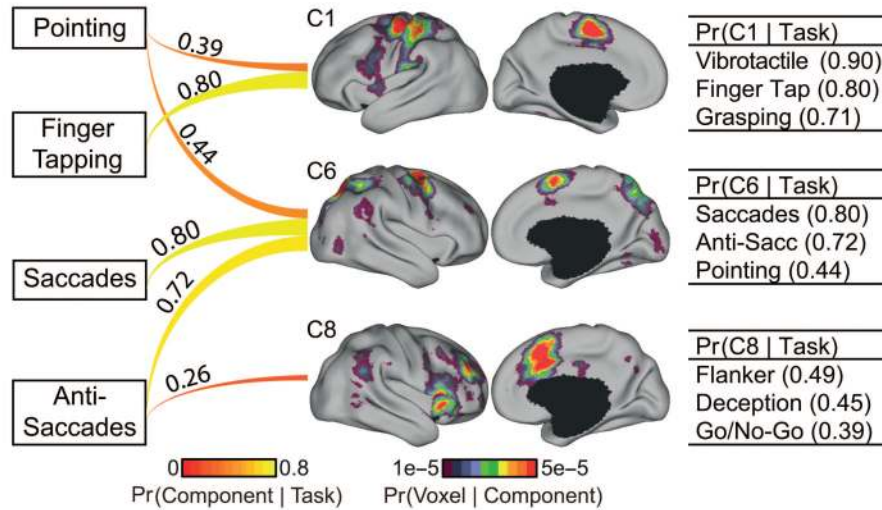
Shared and Divergent Components of Tasks Involving Motor Processing

While the previous subsection focused on tasks strongly associated with individual components (i.e., columns of Fig. 3), it is also instructive to consider the shared and divergent components recruited across tasks (i.e., rows of Fig. 3). To demonstrate how our approach might reveal the relationships among different tasks, the differential recruitment of cognitive components by 4 BrainMap-defined motor-related tasks—"Pointing," "Finger Tapping," "Saccades," and "Anti-Saccades"—was explored (Fig. 4*a*). The 4 tasks were chosen for illustration and are not meant to be exhaustive of all tasks that involve motor processing. Other examples can be readily found by examining Figure 3 and the publicly available model estimates.

Shared and Divergent Components of Tasks Involving Cognitive Control

We considered the differential recruitment of cognitive components by 8 BrainMap-defined cognitive control tasks. The choice of tasks was again not meant to be exhaustive but rather to illustrate shared and divergent components recruited across commonly used cognitive control tasks. Our 12-component estimate indicated that these tasks heavily recruited components C4, C5, C6, C8, and C9 to different degrees (Fig. 4*b*). Components C8 and C9 were the most heavily recruited.
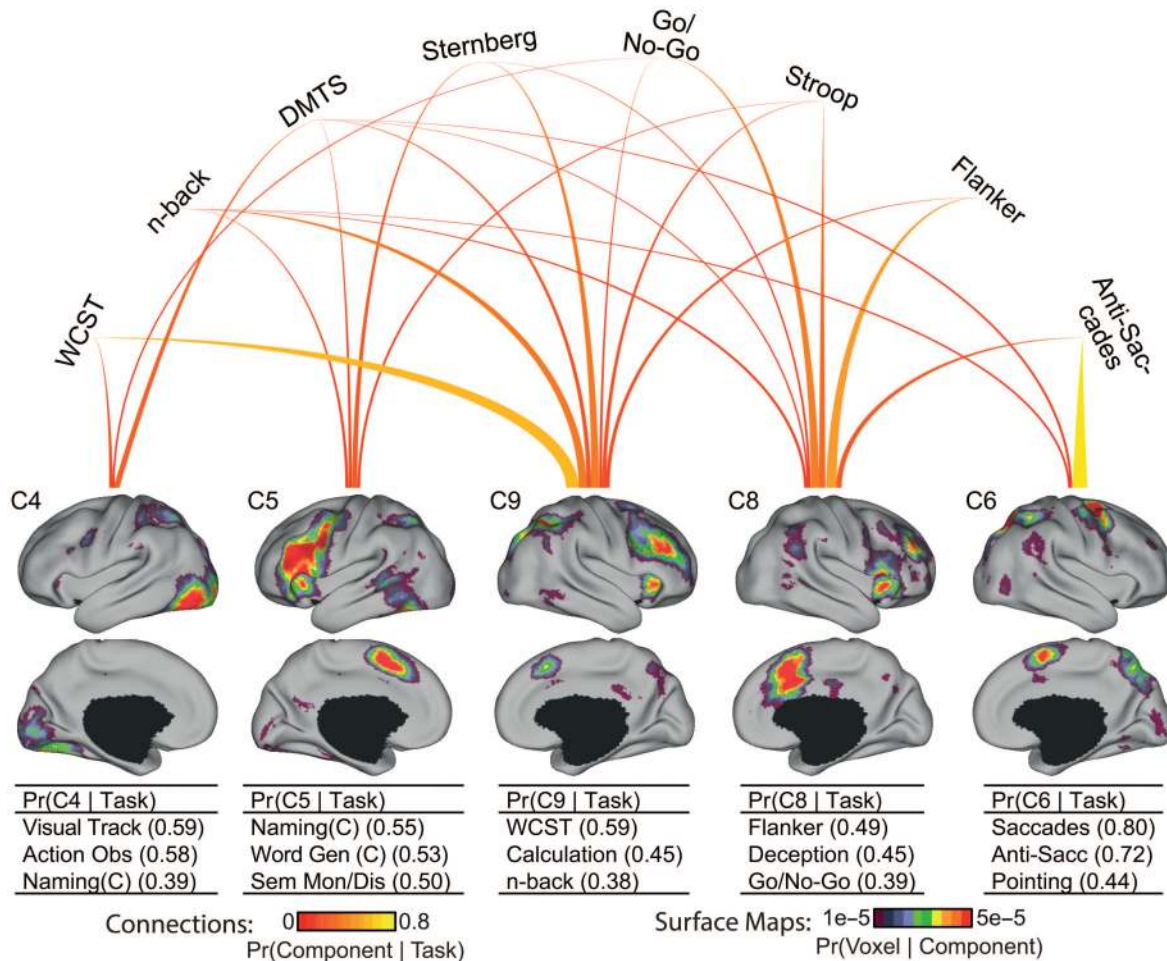
Figure 4. Shared and divergent components of tasks involving motor processing or cognitive control. (*a*) Shared and divergent components of tasks involving motor processing. The 4 motor-related tasks have high probability of recruiting components C1, C6, and C8. Each line connects 1 task with 1 component. The thickness and brightness of the lines are proportional to the magnitude of Pr(component | task). The 3 tasks most likely to recruit these components are shown on the right. The numbers in the brackets correspond to Pr (component | task); the numbers can add up to >1 because we are showing Pr(component | task) and not Pr(task | component). The "Pointing" task recruited components C1 and C6. The "Anti-Saccade" task recruited components C6 and C8. (*b*) Shared and divergent components of tasks involving cognitive control. Format follows (*a*). The 8 cognitive control tasks have high probability of recruiting components C4, C5, C9, C8, and C6. Components C8 and C9 were the most heavily recruited components. Wisconsin Card Sorting Test (WCST), n-back, Delayed Match-to-Sample (DMTS), and Sternberg preferentially recruited component C9, whereas Go/No-Go, Stroop, and Flanker preferentially recruited component C8.
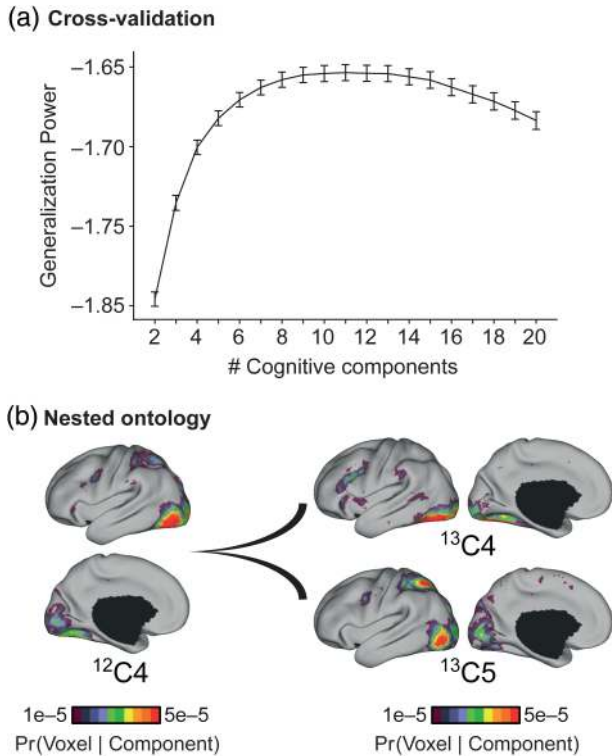
(a) Cross-validation

(b) Nested ontology

Figure 5. Number of cognitive components. (*a*) Generalization power plotted as a function of the number of estimated cognitive components. Generalization power is flat from 8 to 14 components. (*b*) Illustration of the division of visual component into dorsal and ventral visual streams as the number of estimated components was increased from 12 to 13. Here, component ^{12}C4 had high likelihood of activating occipital, superior parietal, and inferior temporal cortices. In contrast, component ^{13}C4 had high likelihood of activating occipital and inferior temporal cortices, whereas component ^{13}C5 had high likelihood of activating occipital and superior parietal cortices. The average of the Pr(voxel | component ^{13}C4) and Pr(voxel | component ^{13}C5) is strongly correlated with Pr(voxel | component ^{12}C4) (see Supplementary Fig. 4), suggesting that the 13-component estimate arises from the subdivision of component ^{12}C4 into components ^{13}C4 and ^{13}C5. This "nested ontology" phenomenon was observed for the flat part of the generalization power curve and in fact beyond it from 6 to 16 components. The flat generalization power and nested ontology suggest that estimates with different number of cognitive components might provide distinct insights into the organization of cognitive components. See Supplementary Figure 4 for quantification of the nested ontology. Supplementary Figure 5 and Table 1 illustrate other component fractionations.

Nested Ontology

An important model parameter is the number of cognitive components. Cross-validation was used to quantify the model generalization power as a function of the number of cognitive components. Generalization power was flat from 8 to 14 components (Fig. 5*a*).

We explored the possibility that components divided into subcomponents as the number of components increased from 2 to 20. The correlation values in Supplementary Figure 4 suggest that from 6 to 16 components, additional components emerged as subdivisions of lower-order components, corresponding to a nested ontology. Examples from 10 to 14 components are illustrated (Fig. 5*b* and Supplementary Fig. 5; Supplementary Table 1).

The flat generalization power and nested ontology suggest that estimates derived from different numbers of cognitive components might provide distinct insights. Indeed, in the 11-component estimate, components C8 and C9 from the 12-component estimate were merged as a single component (Supplementary Fig. 5*b*; Supplementary Table 1). Given the additional insights
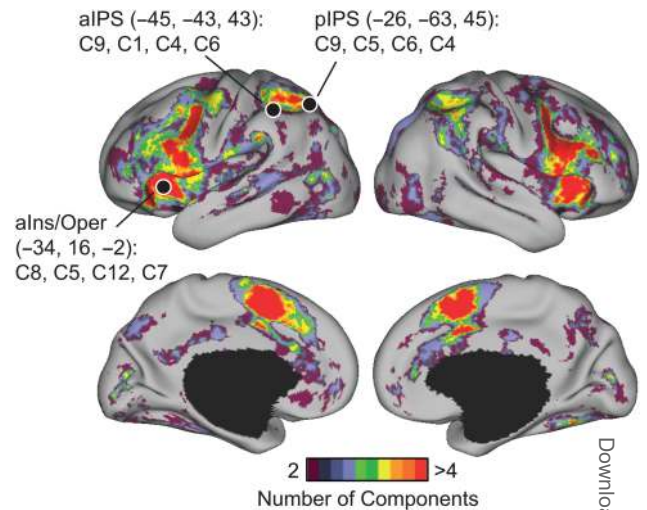

Figure 6. Functional heterogeneity within functionally flexible regions. The figure shows cortical regions participating in multiple cognitive components of the 12-component estimate. Functionally flexible regions were mostly located in the frontal and parietal lobes. These functionally flexible regions are functionally heterogeneous. For example, the top 4 components activating an anterior insula/operculum (aIns/Oper) region (−34, 16, −2) were C8, C5, C12, and C7, with corresponding Pr(component | aIns/Oper) equal to 0.20, 0.19, 0.17, and 0.15, respectively. In contrast, the top 4 components activating an aIPS region (−45, −43, 43) were C9, C1, C4, and C6, with corresponding Pr(component | aIPS) equal to 0.23, 0.21, 0.16, and 0.13, respectively. There was heterogeneity even within a functionally flexible zone, for instance across the IPS. For example, in contrast to aIPS, the top 4 components activating a pIPS region (−26, −63, 45) were C9, C5, C6, and C4, with corresponding Pr(component | pIPS) equal to 0.36, 0.24, 0.20, and 0.08, respectively. The Desikan–Killiany atlas (Desikan et al. 2006) was used to guide the labeling of the regions aIns/Oper, aIPS, and pIPS.

that C8 and C9 provide about cognitive control tasks (previous subsection), we focus on the 12-component estimate in the remaining portion of this paper. Model estimates for 10 to 14 components are publicly available.

Functionally Flexible Regions Are Functionally Heterogeneous

To quantify the functional flexibility of cortical regions, the number of components where Pr(voxel | component) $\geq 1e − 5$ was computed for each voxel (Fig. 6). Experiments with other thresholds than $1e − 5$ yielded similar results, that is, functionally flexible regions were consistently located in the frontal and parietal lobes, including anterior insula, anterior mid-cingulate cortex, intraparietal sulcus, superior parietal lobule, and posterior (medial and lateral) frontal cortex. Furthermore, an alternative measure of functional flexibility (unnormalized entropy) resulted in a very similar map (Supplementary Fig. 6; $r = 0.88$).

The set of flexible regions we identified overlapped considerably ($r = 0.45$; $P \approx 0$) with the MD system (Supplementary Fig. 7; Duncan 2013; Fedorenko et al. 2013). However, the present results also suggest that these functionally flexible regions are functionally heterogeneous. For example, the top 4 components activating a left anterior insular/opercular (aIns/Oper) region were C8, C5, C12, and C7, whereas the top 4 components activating a left anterior intraparietal sulcal (aIPS) region were C9, C1, C4, and C6 (Fig. 6). Therefore, the 2 regions were flexible for completely different components.

Even neighboring regions showed such differences. For example, the top 4 components activating a left posterior intraparietal sulcal (pIPS) region were C9, C5, C6, and C4 (Fig. 6). Therefore, while both aIPS and pIPS regions were functionally flexible for similar components, they still exhibited distinct functional profiles.

One caveat is that the functional flexibility inferences are likely overestimates because of inter-subject and inter-study smoothing inherent to coordinate-based meta-analyses. For example, there were hints of functional differentiations within posterior medial frontal cortex (Supplementary Fig. 8) that were not obvious in other functionally flexible regions. In contrast, functional specificity inferences in the next section are likely underestimates.

Islands of Specialization throughout Association Cortex

To explore functional specialization with respect to the identified components, the functional specificity measure was computed for the entire cerebral cortex (Supplementary Fig. 9). We focus here on the interpretation of lateral frontal (Fig. 7) and parietal (Fig. 8) cortices. Only regions with statistically significant (FDR-corrected $q < 0.05$) functional specificity of at least 2 are shown.
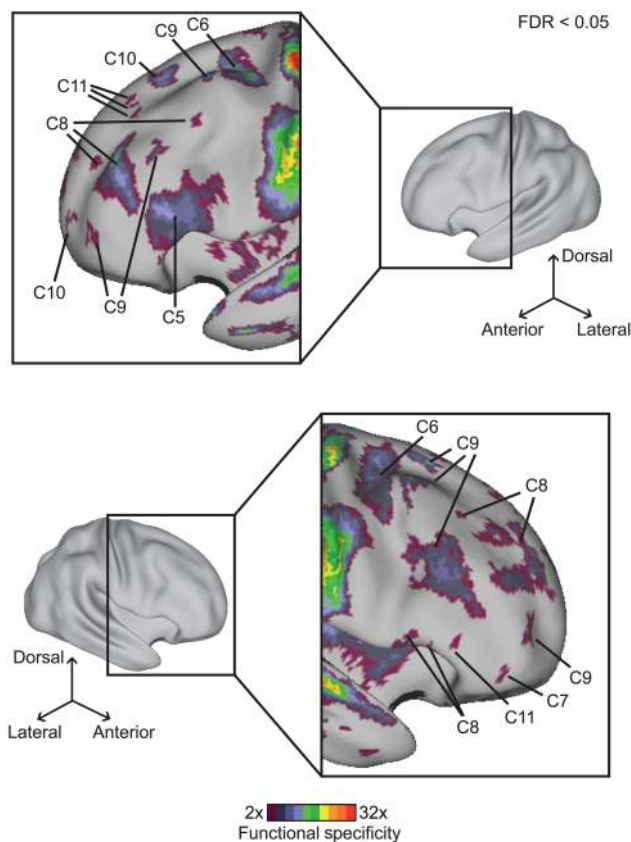

Figure 7. Functional specificity in lateral frontal cortex for the 12-component estimate. A functional specificity value of 2 at a vertex implies that for an activated vertex, the top component would be twice as likely as the second most likely component to be recruited. Therefore, a functional specificity of 2 suggests at least some degree of functional specialization. Only regions with statistically significant (corrected for multiple comparison for entire cerebral cortex, FDR $q < 0.05$) functional specificity of at least 2 are shown. The somato-motor cortex exhibited higher functional specificity than the lateral frontal cortex. Nevertheless, 7 components exhibited significant specificity, demonstrating functional segregation in lateral frontal cortex. Note that the color scale is logarithmic.

Lateral Frontal Specialization

The somato-motor and auditory cortices exhibited significantly higher functional specificity than the lateral frontal cortex. Nevertheless, 7 components exhibited significant specificity in the lateral frontal cortex (Fig. 7), demonstrating considerable functional segregation within this region.

Multiple zones selective for either component C8 or C9 populated large portions of lateral frontal cortex, extending from posterior frontal regions to the frontal pole. As discussed in the previous sections, components C8 and C9 were heavily recruited by cognitive control tasks.

The right IFG and frontal operculum were specific for component C8, whereas the left IFG was specific for component C5. The junction between the precentral and superior frontal sulci was specific for component C6. Finally, the most dorsal aspect of left lateral frontal cortex was functionally specific for components C10 and C11.

Lateral Parietal Specialization

Seven components exhibited significant specificity in the lateral parietal cortex (Fig. 8). The 7 components overlapped with, but were not the same as those in lateral frontal cortex. In particular, bilateral intraparietal sulci were specialized for component C9, but only a small region in the left parietal operculum was specialized for component C8. Therefore, only 1 of the 2 major cognitive control components was strongly anchored in lateral parietal cortex.

Other specializations include component C10 in the inferior parietal cortex and component C6 in the superior parietal cortex. There were also small regions in right superior parietal cortex specialized for components C1, C4, and C7. Regions in
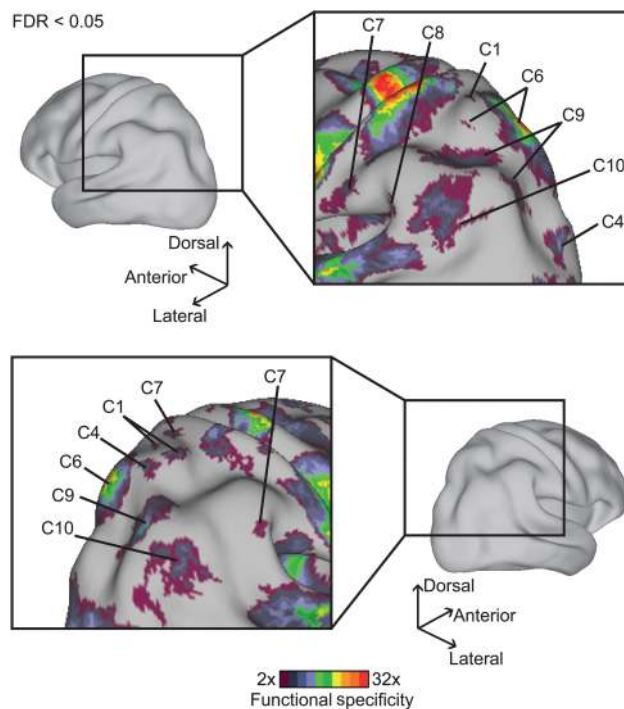

Figure 8. Functional specificity in lateral parietal cortex for the 12-component estimate. Format follows Figure 7. The somato-motor and auditory cortices exhibited higher functional specificity than the lateral parietal cortex. Nevertheless, 7 components exhibited significant specificity, demonstrating functional segregation in lateral parietal cortex.

the parietal operculum and anterior inferior parietal cortex were specialized for component C7.

The functional specificity measure proposed here aimed to capture the notion that specificity implies some degree of functional exclusion. A region specific for a particular function *X* implies that the region is involved in function *X more* than some other function *Y*. Therefore, the functional specificity measure is also somewhat conservative. For example, some might consider a voxel activated by 2 components with equal probability of 0.5 to be functionally specific. Our quantitative measure does not consider such a voxel to be functionally specific.

Given that the functional specificity measure is a ratio of the most likely and second most likely component, one might be concerned that a region whose most likely component is rather improbable may be considered functionally specific if the second most likely component is even less improbable, such as the probability of the most likely component is 0.2 and the probability of the second most likely component is 0.1. Such cases are rare. Indeed, the map corresponding to the highest Pr(component | voxel) is very similar to the functional specificity estimate ($r = 0.89$).

Functional Specificity Estimates Are Robust to Analysis Choices

To ensure that the functional specificity estimates were robust, the data were re-analyzed using a simple procedure (see Methods), which simulated traditional meta-analyses (e.g., Duncan and Owen 2000; Shackman et al. 2011) that categorized tasks into distinct groups a priori. Briefly, we computed the probability that the top *K* tasks of each component would activate each cortical vertex: Pr(vertex | top *K* tasks). The islands of specificity in lateral frontal and parietal cortices (Figs. 7 and 8) were then used as ROIs to determine, for each ROI, whether the component identified in the previous analysis matched the component with the highest Pr(vertex | top *K* tasks) within the ROI.

This analysis ignored the possibility that tasks within the same group might recruit distinct processes (in addition to common processes) or that tasks in different groups might share common processes. For example, since "Covert Naming" is one of the top 4 tasks recruiting components C4 and C5 (Table 1), activation foci from "Covert Naming" studies will be counted toward both components for values of *K* from 4 to 10. In contrast, under our model (Fig. 1), activation foci from "Covert Naming" studies will be shared among components C4, C5, and other components recruited by "Covert Naming." More importantly, the Pr(vertex | top *K* tasks) was computed per vertex (see Methods) and therefore does not sum to 1 over the brain. This is in contrast to Pr(voxel | component) estimated by the author-topic model, which sums to 1 over all voxels. Given the above-mentioned differences, agreement with the author-topic model is not obligate.

We initially performed this analysis for *K* = 5. For 29 of the 41 functionally specific lateral frontal and parietal ROIs, the most likely component (as identified in Figs. 7 and 8) had the highest Pr(vertex | top 5 tasks) within the respective ROIs. For 6 of the remaining 12 ROIs, the most likely component had the second highest Pr(vertex | top 5 tasks). Therefore, our quantitative functional specificity measure and this analysis (Supplementary Fig. 10) were highly consistent ($P < 1e − 5$),

indicating that the functional specificity estimates accurately reflected the BrainMap data. Repeating the analysis with different values of *K* yielded similar results. For 37 of the 41 ROIs, the most likely component identified by the author-topic model had the highest Pr(vertex | top *K* tasks) for at least one value of *K*.

Regions Specialized for the Same Cognitive Components Are Strongly Connected

The above-mentioned results suggest that the functional specificity estimates likely reflect true properties of the BrainMap database. As the distribution of activation foci and tasks is non-uniform, a separate resting-state fMRI analysis was employed, which does not suffer from this bias. Importantly, the resting-state analysis was performed on a surface coordinate system without any volumetric smoothing. This also alleviates concerns that the complex pattern of functional specificity may have arisen from the smoothing of activation results across cortical folds.

We first tested the hypothesis that cortical regions specialized for the same cognitive components would be more strongly coupled than those specialized for different components. Because of their complex pattern, the lateral frontal regions specialized for components C8 and C9 constituted a challenging test set (Fig. 9a). Resting-state correlations among lateral frontal islands specialized for component C8 were stronger than their correlations with lateral frontal islands specialized for component C9 ($P < 1e − 184$). Similarly, functional coupling among lateral frontal islands specialized for component C9 was stronger than their coupling to lateral frontal islands specialized for component C8 ($P < 1e − 75$).

Furthermore, across the entire cerebral cortex, functional coupling among cortical regions specialized for the same component was stronger than among those specialized for different components ($P \approx 0$). Therefore, the cognitive components reflect meaningful brain organization, which persists even in the resting state (also see Smith et al. 2009; Mennes et al. 2013; Krienen et al. 2014). These results also suggest that regions specialized for the same component function as functionally coupled networks, partially isolated from other components.
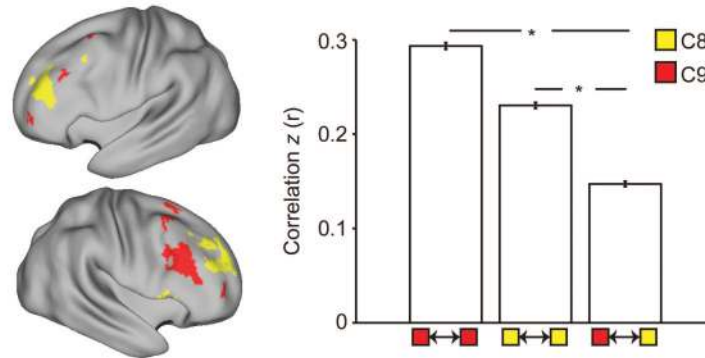
Connectivity Patterns Predict the Functional Heterogeneity of Flexible Regions

We next tested the hypothesis that functional heterogeneity across functionally flexible regions might relate to distinct connectivity patterns (Goldman-Rakic 1988; Passingham et al. 2002; Saygin et al. 2012). The resting-state functional connectivity between each functionally flexible region and other functionally specialized regions varied proportionally to the probability of the individual components activating the functionally flexible region (average $r = 0.75$, $P \approx 0$; Fig. 9b). In other words, a functionally flexible region with high likelihood of being activated by component X tends to exhibit strong coupling with other regions specialized for component X. Therefore, functionally flexible regions might serve to integrate information from the specialized regions of one or more components.

Discussion

By employing a novel data-driven approach on one of the largest meta-analytic data sets available, we estimated a latent
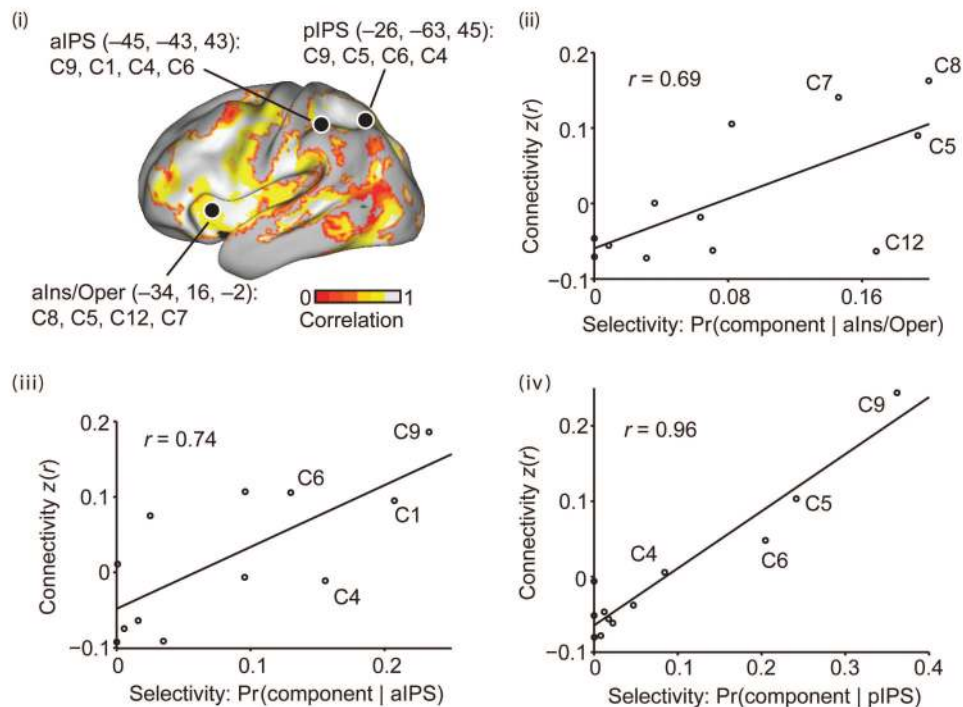
Figure 9. Intrinsic organization of functionally specialized and flexible regions. (*a*) Regions specialized for the same cognitive components are strongly connected. Yellow regions correspond to lateral frontal zones specialized for component C8. Red regions correspond to lateral frontal zones specialized for component C9. Functional coupling among lateral frontal zones specialized for component C8 was stronger than their coupling with zones specialized for component C9 ($P < 1e - 184$). Similarly, functional coupling among lateral frontal zones specialized for component C9 was stronger than their coupling with zones specialized for components C8 ($P < 1e - 75$). Therefore, components function as isolated specialized networks. Asterisks indicate the statistical tests performed. (*b*) Connectivity patterns of functionally flexible regions are correlated with their selectivity for cognitive components. (*b$_i$*) The colored regions are functionally flexible for at least 2 components (c.f. Fig. 6). The overlay corresponds to the correlation between the selectivity (Pr (component | functionally flexible region)) and the functional connectivity of the functionally flexible region and specialized regions of individual components. Average correlation across all functionally flexible regions = 0.75 ($P \approx 0$). The high positive values suggest that a functionally flexible region with high likelihood of being activated by component X tends to have stronger connectivity with regions specialized for component X. (*b$_{ii-iv}$*) Example scatterplots for the 3 functionally flexible regions from Figure 6: (*b$_{ii}$*) aIns/Oper, (*b$_{iii}$*) aIPS, and (*b$_{iv}$*) pIPS. Therefore, the connectivity patterns of functionally flexible regions were consistent with their selectivity to individual cognitive components. Flexible regions might integrate information from isolated specialized networks.

cognitive structure and its cortical topography without a priori categorization of tasks. Our results suggest a complex pattern of functionally specialized and flexible regions distributed across association cortex. In follow-up analyses using resting-state data, regions functionally specialized for the same components were found to be strongly coupled, suggesting they function as partially isolated networks. Functionally flexible regions are heterogeneous, that is, they support multiple components, but each does so to different degrees. This heterogeneous selectivity of the flexible regions is predicted by the

functional coupling between flexible and specialized regions. One possibility is that functionally flexible regions support binding or integrating specialized brain networks that, in turn, contribute to the execution of multiple and varied tasks.

Nested Latent Cognitive Structure

A core result in this work is the estimation of a set of latent cognitive components that underlie the patterns of brain activation observed in task-based functional imaging studies.

Different tasks recruited overlapping cognitive components, and different components activated common and distinct brain regions across distributed cortical and subcortical structures. Cortical regions with the same specialization were strongly coupled, functioning as a distributed but coherent component. These observations bolster the proposal that the relevant units of brain function are networks of brain regions (Goldman-Rakic 1988; Mesulam 1990; McIntosh 2000; Yeo et al. 2011). While differentiated functions among regions of the same cognitive component are expected, this perspective emphasizes that complex brain functions arise from emergent network properties.

The model used here requires specifying the number of components. Analysis revealed a nested ontology of components across different solutions. For example, the 12-component estimate of C4 (^{12}C4) divided into the 13-component estimates of C4 (^{13}C4) and C5 (^{13}C5). The remaining 11 components were almost identical across the 2 solutions. The average correlation value for this hypothesized split was 0.95 (Supplementary Fig. 4) indicating the subdivision was excellent. Based on the activation patterns (Fig. 5b) and the top tasks likely to recruit the components (Supplementary Table 1), the fractionation of component ^{12}C4 into components ^{13}C4 and ^{13}C5 may reflect the segregation of visual processing into dorsal and ventral visual streams. Therefore, the nested ontology revealed meaningful fractionations of components.

We recognize that the estimated ontology is a "conditional ontology" because the components we describe are those that can be discovered through applying the author-topic model to the BrainMap database and the associated paradigm classes. An important feature of this work is that it reveals the cognitive structure and network properties through the probabilistic use of an existing (fairly informal) taxonomy (paradigm classes) and their respective activation patterns. That the resting-state analyses were able to corroborate properties of these patterns helps to validate the approach.

Shared and Divergent Components across Task Categories

The identification of tasks that had a high probability of activating each component provides quantitative insight into the putative function or process of each component (Figs. 2a and 3; Table 1). Critically, the model revealed relationships among different sets of tasks. We next consider two examples from different domains.

Shared and Divergent Components of Tasks Involving Motor Processing

The differential recruitment of cognitive components by 4 BrainMap-defined motor tasks ("Pointing," "Finger Tapping," "Saccades," and "Anti-Saccades") was explored (Fig. 4a). We have previously suggested that component C1 is involved in touch or hand motion, and component C6 is involved in eye movement or spatial attention. The "Pointing" task recruited components C1 and C6, consistent with the notion that pointing at an object involves hand-eye coordination. The "Anti-Saccade" task requires suppressing the pre-potent response driven by the visual cue and making a saccade in the opposite direction. The recruitment of component C8 (in addition to C6) by the "Anti-Saccades" task is consistent with the notion that component C8 is related to inhibition of pre-potent responses (Miyake et al. 2000) or response conflict (Duncan and Owen

2000). Thus, "Anti-Saccade" differs from "Pointing," "Finger Tapping," and "Saccades" by additionally recruiting a non-motor component.

Shared and Divergent Components of Tasks Involving Cognitive Control

Since the association cortex plays an important role in cognitive control operations (Dosenbach et al. 2006; Corbetta et al. 2008; Duncan 2013), the differential recruitment of cognitive components by 8 BrainMap-defined cognitive control tasks was considered. These tasks heavily recruited components C4, C5, C6, C8, and C9 (Fig. 4b). The most heavily recruited components were C8 and C9. As mentioned earlier, C8 might be related to inhibition or response conflict. Consistent with this hypothesis, the "Stroop" task preferentially recruited component C8 relative to C9 (Fig. 3). Component C9 was most strongly associated with "Wisconsin Card Sorting Test," "Counting/Calculation," and "n-back," suggesting a link to tasks engaging working memory. Consistent with this speculation, "Sternberg" and "Delayed Match to Sample" tasks preferentially recruited C9 relative to C8 (Fig. 3). All 5 components had high probability of activating distinct portions of the association cortex, hinting at functional specialization. Overlapping activation between components was also evident, suggesting the presence of functionally flexible regions, at least at the resolution of our derived components.

The differential recruitment of C8 and C9 echoes previous data-driven dissociation of cognitive control processes (e.g., Miyake et al. 2000; Dosenbach et al. 2007; Lenartowicz et al. 2010). However, alternative interpretations are possible. For example, the activation pattern of component C8 resembles the cinguloopercular network, thought to be involved in the stable maintenance of task sets, whereas the activation pattern of component C9 resembles the frontoparietal network that might be involved in adaptive online control (Dosenbach et al. 2007).

A Spectrum of Specialization and Flexibility across Association Cortex

While association cortex has long been known to underpin flexible behavior, the ontology of cognitive functions and their instantiation in the brain continues to be elaborated. For example, whether the left inferior frontal cortex participates exclusively in linguistic semantic processes or instead supports domain-general functions remains an active topic of investigation (Thompson-Schill et al. 1997; Wagner et al. 2001; Gold and Buckner 2002; Devlin et al. 2003; Koechlin et al. 2003; Badre et al. 2005; Fedorenko et al. 2012; Clos et al. 2013). More broadly, it has been proposed that certain prefrontal and parietal regions possess flexible processing capabilities and may be recruited across multiple "cognitive demands" (Duncan 2001; Wise 2008; Cromer et al. 2010; Fitzgerald et al. 2011; Duncan 2013; Rigotti et al. 2013).

Several frontal and parietal regions were activated by multiple cognitive components, consistent with reports emphasizing prefrontal and parietal flexibility (Duncan 2001; Spreng et al. 2010; Cole et al. 2013; Duncan 2013; Fedorenko et al. 2013). These flexible regions included the intraparietal sulcus, which contained an anterior region involved in at least 4 cognitive components, as well as the anterior insula/operculum, superior parietal lobule, and posterior frontal cortex.

Conversely, highly specialized zones were also distributed throughout frontal and parietal cortices, compatible with

some functional attribution studies (e.g., Aron et al. 2004; Fedorenko et al. 2012). For example, both left SPL and IFG were highly specialized with Pr(C6 | left SPL) ≈ 0.9 and Pr(C5 | left IFG) ≈ 0.6.

Other regions exhibited intermediate specialization. For example, the right IFG appears moderately specialized with Pr (C8 | right IFG) ≈ 0.4 (functional specificity measure ≈ 3). As another example, a moderately flexible region within left posterior lateral frontal cortex was associated with C5 and C9: Pr (C5 or C9 | left posterior lateral frontal cortex) ≈ 0.6.

In considering our results, there are important caveats. The inter-subject and inter-study smoothing inherent to coordinate-based meta-analyses likely bias the present flexibility and specificity metrics in opposite ways. Flexibility could be overestimated if adjacent, differentially specialized regions were smoothed together. This could further impact the findings regarding the functional heterogeneity of flexible regions if these regions are adjacent to neighbors with different specializations. In contrast, functional specificity inferences are likely underestimates. The independent resting-state analysis utilizes surface-based registration that partially mitigates the effect of inter-study smoothing and minimizes inter-subject variability compared with volumetric registration (Fischl et al. 2008; Yeo et al. 2010; Van Essen et al. 2012). Nevertheless, within-subject multi-task analyses (e.g., Fedorenko et al. 2012) will be necessary to assess the impact of smoothing on metrics for flexibility and specificity.

By aggregating evidence across thousands of experiments, our meta-analysis reveals multiple association zones ranging from being highly specialized to highly flexible. Our data suggest some properties of these zones but leave unanswered the broader question of how they form or whether there are simplifying organizational principles to the complex topography.

Integrated versus Segregated Processing

Since cortical regions specialized for distinct components were weakly coupled, a critical issue concerns how information is integrated across components. We found that flexible regions were more strongly coupled in the resting state to specialized regions of those cognitive components they were likely to participate in, suggesting that the functionally flexible regions may play important integrative roles. The interactions within and between components may enable the human association cortex to facilitate or perform a multitude of different cognitive tasks.

An influential perspective of information processing in the primate cerebral cortex is that of sensory information elaborated and refined by a processing hierarchy (Ungerleider and Desimone 1986; Felleman and Van Essen, 1991). Streams of information from different sensory modalities converge upon and receive feedback from heteromodal association cortex, where they are integrated to create coherent experience and drive behavior (Mesulam 1998). Consequently, one might expect many association regions to be linked with or display mixed selectivity to multiple cognitive domains (Rigotti et al. 2013). Other association regions may be largely nonspecific to sensory domains (Buckner and Krienen 2013). Consistent with these perspectives, our results suggest that the association cortex is less functionally specific than sensory cortex and that functionally flexible regions are largely located in association cortex (also see Yeo et al. 2014).

The pioneering work of Pandya and Kuypers (1969) and Jones and Powell (1970) established the anatomical basis for viewing PFC as the terminus of a variety of sensory afferents. Notably, they did not find a single PFC region where the full diversity of sensory streams converge (Goldman-Rakic 1988). The present results are consistent with their analyses. While there were functionally flexible zones in association cortex, the flexible regions were functionally heterogeneous. Moreover, functionally specific zones were apparent within association cortex. The observed spectrum of specificity reinforces the notion that the moniker "association cortex" does not describe a uniform computational entity. The degree of specialization may vary considerably between distinct regions of association cortex, and functional models should consider this heterogeneity.

Association cortex that is functionally specialized in some parts while heterogeneous and functionally flexible in others may reconcile prominent frameworks offered previously. In particular, distributed and segregated information processing may not be incompatible with hierarchical and integrative processing (Goldman-Rakic 1988; Mesulam 1998; Power et al. 2011; Yeo et al. 2011, 2014; Buckner and Krienen 2013). The flexible association regions might support a core processing capacity by binding or integrating segregated brain networks specialized for distinct functions (also see Damasio 1989; Bassett et al. 2013; Markov et al. 2013).

A Heterogeneous, Multi-Functional Brain System

Our analyses revealed a set of functionally flexible regions that have been implicated in a multitude of functions (Menon and Uddin 2010; Shackman et al. 2011) and may play important integrative roles (Miller and Cohen 2001; Duncan 2013; Shenhav et al. 2013). In terms of spatial overlap, the flexible regions were consistent with the MD system (Duncan 2013; Fedorenko et al. 2013).

Fedorenko et al. (2013) demonstrated that the MD regions are activated across diverse task domains ("Math," "Spatial Working Memory," "Verbal Working Memory," "Stroop," "Verbal MSIT," and "Numeric MSIT"). Based on Figure 3, the tasks employed by Fedorenko et al. (2013) likely recruited 2 (C8 and C9) of our 12 components to different degrees. As such, our meta-analysis permits an expanded assessment of the cognitive domains associated with the MD system (Fig. 6). For example, a functionally flexible region within intraparietal sulcus supports component C9, but not C8. Conversely, a functionally flexible region near the anterior insula/operculum supports component C8, but not C9.

Functionally flexible regions can differ in the assortment of functions with which they associate. For example, an intraparietal sulcal region and an anterior insular/opercular region were associated with different cognitive components. In addition, there were variations in functional profiles even within a flexible zone (e.g., within intraparietal sulcus). Hence, the MD system, while serving multiple functions, might itself be functionally heterogeneous (also see Hampshire et al. 2012).

Such heterogeneity presumably arises, in part, from distinct connectivity profiles across the MD regions (Passingham et al. 2002). One possibility is that the flexible regions may be performing similar functions, but differences among regions may lie in the nature of the information being operated upon (Goldman-Rakic 1988). Consistent with this hypothesis, the flexible regions

were more strongly coupled to specialized regions of those cognitive components that they were likely to participate in. This tight relationship between selectivity and connectivity across large expanses of the cerebral cortex extends previous work focusing on fusiform cortex (Saygin et al. 2012).

Our model does not allow differentiation between existing functional accounts of the functionally flexible regions. For instance, Duncan (2010) suggests, "the essential function of the MD system might lie in separating, organizing, storing and controlling the parts of complex, intelligent mental activity." Dosenbach et al. (2007) proposes that separable networks (whose regions overlap with MD regions) serve 2 dissociable functions: 1) the stable maintenance of task sets and 2) adaptive online control. The present results are consistent with both accounts insofar as the flexible and heterogeneous regions we identified overlap with those discussed in these prior accounts, and that cognitive control tasks tend to recruit these regions. However, with the present approach, we can only speculate as to the specific functions subserved by the components.

The estimated functionally flexible regions overlap with regions reported to be frequently activated in the neuroimaging literature (Poldrack 2011; Behrens et al. 2013). Given the overlap between the functional flexibility estimate and the MD system from individual subjects (Fedorenko et al. 2013), the non-uniform spatial distribution of foci in the literature might not reflect a biased selection of tasks. Instead, the non-uniform spatial distribution may reflect that functionally flexible regions are activated across a wide range of cognitive domains, possibly due to their integrative roles.

Related Neuroimaging Meta-Analyses

The present work builds on prior meta-analyses that have investigated functional specialization (e.g., Rottschy et al. 2012; Clos et al. 2013) and flexibility (e.g., Binder et al. 2009; Shackman et al. 2011; Niendam et al. 2012) in the human brain. One novel aspect of the present work—derived from the use of a data-driven mathematical formalization of the relationship between tasks, cognitive components, and brain regions—is that a broad task- and brain-space could be simultaneously examined. Typically, analyses are limited to specific brain regions (e.g., anterior mid-cingulate cortex or DLPFC) or particular cognitive domains (e.g., semantic memory). Here, the entire human cerebral cortex was considered across all task categories in the BrainMap database.

Specifically, prior meta-analyses a priori categorize tasks into cognitive domains by appealing to specific cognitive theories (e.g., Kang et al. 2011; Salimi-Khorshidi et al. 2011; Yue et al. 2012). The present approach allows automatic estimation of cognitive components without prior membership constraints. While some meta-analyses utilize clustering approaches that do not require a priori categorization of tasks, they typically assume that the tasks belong to distinct non-overlapping categories (Laird et al. 2011) or that each brain region belongs to a single "cluster" (Cieslik et al. 2013; Clos et al. 2013). Here, we sought to formally model the classic notion that a particular task recruits multiple cognitive components supported by multiple brain regions (Walton and Paul 1901; Posner et al. 1988).

Model Considerations

The many-to-many mapping between tasks, cognitive components, and brain regions may partly reflect differences across experiments within a task category, involving dimensions such as stimulus modality (e.g., visual vs. auditory) and task difficulty (e.g., "3-back" > "2-back" vs. "1-back" > "0-back"). Future analyses incorporating additional, objectively defined Brain-Map meta-data (e.g., "stimulus modality") may resolve these variations and further refine estimates.

The sharing of cognitive components across tasks in the hierarchical Bayesian model can improve the estimation of components recruited by tasks poorly represented in the database or literature. Components of poorly represented tasks can still be accurately estimated if the components are also recruited by more popular tasks or if many poorly represented tasks recruit the same component. This is a well-known computational advantage of this kind of model (Blei et al. 2003).

It is important to emphasize that in this work, the terms "flexibility" and "specificity" refer to the operational definitions used in the model and are agnostic to the cognitive *functional description* of a particular component or region. For example, a flexible region associated with cognitive control, language and visual processing might be alternatively described as supporting a *specific* abstract function (e.g., "modality-dependent control"), or as *flexibly* performing different functions in different contexts. As such, functional flexibility may indicate higher-level functions that are either more abstract or coordinative in nature. Furthermore, there is likely a hierarchical nesting of cognitive descriptions, similar to what was observed in the nesting of estimated components.

In addition, it is important to interpret the specialization and flexibility maps with respect to the estimated components, rather than treating the maps as absolutes. For example, it would have been impossible to find regions specialized for distinct cognitive control components using the 11-component estimate because the two cognitive control components in the 12-component estimate are merged in the 11-component estimate. As another example (Supplementary Fig. 9), functional specificity estimates are similar across the 12-component and 13-component estimates; the Pearson's correlation between the two maps is 0.76. Differences in functional specificity estimates between 12-component and 13-component estimates arise mostly in the visual cortex. This is because of the division of the visual component into dorsal and ventral visual streams as the number of components increases from 12 to 13. Note that the nested ontology holds from 6 to 16 components (Supplementary Fig. 4). From 6 to 16 components, finer-grained fractionations could yield a diversity of specialized and flexible components, while retaining properties of conserved components of coarser estimates.

The nested property of the estimates suggests that the components are meaningful but also that different levels of confidence surround the different properties of the components. As described earlier, the specific topography of flexibility and specificity foci is expected to vary across estimates. However, the following general principles are expected to apply across estimates: 1) functionally specific regions are more tightly coupled and 2) flexible regions are heterogeneous and connected to specific regions.

A Resource for Further Inquiry

The attribution of functional specialization may be considered at different spatial scales (Henson 2005; Gilbert et al. 2010). For example, at the macro-scale, the occipital cortex can be

described as being specialized for visual processing. At a finer scale, different occipital areas may be distinguished based on their sensitivity to different visual features. At an even finer scale, different visual subregions within areas may be dissociated based on their visual field response (e.g., central vs. peripheral) or sensitivity to visual parameters (e.g., blobs vs. interblobs).

Our work characterized functional specialization at a macroscale. As such, the nested ontology of cognitive components revealed here suggests that future, more refined fractionation of cognitive components could yield finer-grained insights into the organization of brain function. We anticipate that such advances will be realized as additional studies on normal and abnormal brain function are accrued in the BrainMap database. To this end, we provide estimates of cognitive components (https://surfer.nmr.mgh.harvard.edu/fswiki/BrainmapOntology_Yeo2015, last accessed September 12, 2014) that we hope will serve as starting points for future efforts at functional characterization or cross-validation through complementary approaches. For instance, it would be interesting to determine how flexible and specific regions relate to graph theoretic concepts, such as connector hubs (Guimera and Amaral 2005; Bullmore and Sporns 2009).

Funding

Notes

References

Aron AR, Robbins TW, Poldrack RA. 2004. Inhibition and the right inferior frontal cortex. Trends Cogn Sci. 8:170–177.

Badre D, D'Esposito M. 2009. Is the rostro-caudal axis of the frontal lobe hierarchical? Nat Rev Neurosci. 10:659–669.

Badre D, Poldrack RA, Paré-Blagoev EJ, Insler RZ, Wagner AD. 2005. Dissociable controlled retrieval and generalized selection mechanisms in ventrolateral prefrontal cortex. Neuron. 47:907–918.

Bassett DS, Wymbs NF, Rombach MP, Porter MA, Mucha PJ, Grafton ST. 2013. Task-based core-periphery organization of human brain dynamics. PLoS Comp Biol. 9:e1003171.

Bechtel W. 2002. Decomposing the mind-brain: a long-term pursuit. Brain Mind. 3:229–242.

Behrens TE, Fox P, Laird A, Smith SM. 2013. What is the most interesting part of the brain? Trends Cogn Sci. 17:2–4.

Binder JR, Desai RH, Graves WW, Conant LL. 2009. Where is the semantic system? A critical review and meta-analysis of 120 functional neuroimaging studies. Cereb Cortex. 19:2767–2796.

Blei D, Ng A, Jordan M. 2003. Latent Dirichlet allocation. J Mach Learn Res. 3:993–1022.

Buckner RL, Andrews-Hanna JR, Schacter DL. 2008. The brain's default network: anatomy, function, and relevance to disease. Ann NY Acad Sci. 1124:1–38.

Buckner RL, Krienen FM. 2013. The evolution of distributed association networks in the human brain. Trends Cogn Sci. 17:648–665.

Buckner RL, Krienen FM, Castellanos A, Diaz JC, Yeo BTT. 2011. The organization of the human cerebellum estimated by intrinsic functional connectivity. J Neurophysiol. 106:2322–2345.

Bullmore E, Sporns O. 2009. Complex brain networks: graph theoretical analysis of structural and functional systems. Nat Rev Neurosci. 10:186–198.

Choi EY, Yeo BTT, Buckner RL. 2012. The organization of the human striatum estimated by intrinsic functional connectivity. J Neurophysiol. 108:2242–2263.

Cieslik EC, Zilles K, Caspers S, Roski C, Kellermann TS, Jakobs O, Langner R, Laird AR, Fox PT, Eickhoff SB. 2013. Is there "one" DLPFC in cognitive action control? Evidence for heterogeneity from co-activation-based parcellation. Cereb Cortex. 23:2677–2689.

Clos M, Amunts K, Laird AR, Fox PT, Eickhoff SB. 2013. Tackling the multifunctional nature of Broca's region meta-analytically: Co-activation-based parcellation of area 44. NeuroImage. 83:174–188.

Cole MW, Reynolds JR, Power JD, Repovs G, Anticevic A, Braver TS. 2013. Multi-task connectivity reveals flexible hubs for adaptive task control. Nat Neurosci. 16:1348–1355.

Corbetta M, Patel G, Shulman GL. 2008. The reorienting system of the human brain: from environment to theory of mind. Neuron. 58:306–324.

Cromer JA, Roy JE, Miller EK. 2010. Representation of multiple, independent categories in the primate prefrontal cortex. Neuron. 66:796–807.

Damasio AR. 1989. The brain binds entities and events by multiregional activation from convergence zones. Neural Comput. 1:123–132.

Dempster AP, Laird NM, Rubin DB. 1977. Maximum likelihood from incomplete data via the EM algorithm. J Roy Statist Soc Ser B. 39:1–38.

Desikan RS, Ségonne F, Fischl B, Quinn BT, Dickerson BC, Blacker D, Buckner RL, Dale AM, Maguire RP, Hyman BT et al. 2006. An automated labeling system for subdividing the human cerebral cortex on MRI scans into gyral based regions of interest. NeuroImage. 31:968–980.

D'Esposito M, Detre JA, Alsop DC, Shin RK, Atlas S, Grossman M. 1995. The neural basis of the central executive system of working memory. Nature. 378:279–281.

Devlin JT, Matthews PM, Rushworth MF. 2003. Semantic processing in the left inferior prefrontal cortex: a combined functional magnetic resonance imaging and transcranial magnetic stimulation study. J Cogn Neurosci. 15:71–84.

Dosenbach NU, Fair DA, Miezin FM, Cohen AL, Wenger KK, Dosenbach RA, Fox MD, Snyder AZ, Vincent JL, Raichle ME et al. 2007. Distinct brain networks for adaptive and stable task control in humans. Proc Natl Acad Sci. 104:11073–11078.

Dosenbach NU, Visscher KM, Palmer ED, Miezin FM, Wenger KK, Kang HC, Burgund ED, Grimes AL, Schlaggar BL, Petersen SE. 2006. A core system for the implementation of task sets. Neuron. 50:799–812.

Duncan J. 2001. An adaptive coding model of neural function in prefrontal cortex. Nat Rev Neurosci. 2:820–829.

Duncan J. 2010. The multiple-demand (MD) system of the primate brain: mental programs for intelligent behaviour. Trends Cognit Sci. 14:172–179.

Duncan J. 2013. The structure of cognition: attentional episodes in mind and brain. Neuron. 80:35–50.

Duncan J, Owen AM. 2000. Common regions of the human frontal lobe recruited by diverse cognitive demands. Trends Neurosci. 23:475–483.

Eickhoff SB, Bzdok D, Laird AR, Kurth F, Fox PT. 2012. Activation likelihood estimation meta-analysis revisited. NeuroImage. 59:2349–2361.

Fedorenko E, Duncan J, Kanwisher N. 2012. Language-selective and domain-general regions lie side by side within Broca's area. Curr Biol. 22:2059–2062.

Fedorenko E, Duncan J, Kanwisher N. 2013. Broad domain generality in focal regions of frontal and parietal cortex. Proc Natl Acad Sci USA. 110:16616–16621.

Felleman DJ, Van Essen DC. 1991. Distributed hierarchical processing in the primate cerebral cortex. Cereb Cortex. 1:1–47.

Fischl B. 2012. FreeSurfer. NeuroImage. 62:774–781.

Fischl B, Rajendran N, Busa E, Augustinack J, Hinds O, Yeo BTT, Mohlberg H, Amunts K, Zilles K. 2008. Cortical folding patterns and predicting cytoarchitecture. Cereb Cortex. 18:1973–1980.

Fitzgerald JK, Freedman DJ, Assad JA. 2011. Generalized associative representations in parietal cortex. Nat Neurosci. 14:1075–1079.

Fox PT, Laird AR, Fox SP, Fox PM, Uecker AM, Crank M, Koenig SF, Lancaster JL. 2005. BrainMap taxonomy of experimental design: description and evaluation. Hum Brain Mapp. 25:185–198.

Fox PT, Lancaster JL. 2002. Mapping context and content: the BrainMap model. Nat Rev Neurosci. 3:319–321.

Gilbert SJ, Henson RN, Simons JS. 2010. The scale of functional specialization within human prefrontal cortex. J Neurosci. 30:1233–1237.

Gilbert SJ, Spengler S, Simons JS, Steele JD, Lawrie SM, Frith CD, Burgess PW. 2006. Functional specialization within rostral prefrontal cortex (area 10): a meta-analysis. J Cogn Neurosci. 18:932–948.

Gold BT, Buckner RL. 2002. Common prefrontal regions coactivate with dissociable posterior regions during controlled semantic and phonological tasks. Neuron. 35:803–812.

Goldman-Rakic PS. 1988. Topography of cognition: parallel distributed networks in primate association cortex. Ann Rev Neurosci. 11:137–156.

Greve DN, Fischl B. 2009. Accurate and robust brain image alignment using boundary-based registration. NeuroImage. 48:63–72.

Guimera R, Amaral LAN. 2005. Functional cartography of complex metabolic networks. Nature. 433:895–900.

Hampshire A, Highfield RR, Parkin BL, Owen AM. 2012. Fractionating human intelligence. Neuron. 76:1225–1237.

Henson R. 2005. What can functional neuroimaging tell the experimental psychologist? Q J Exp Psychol-A. 58:193–233.

Jones E, Powell T. 1970. An anatomical study of converging sensory pathways within the cerebral cortex of the monkey. Brain. 93:793–820.

Kang J, Johnson TD, Nichols TE, Wager TD. 2011. Meta analysis of functional neuroimaging data via Bayesian spatial point processes. J Am Stat Assoc. 493:124–134.

Koechlin E, Ody C, Kouneiher F. 2003. The architecture of cognitive control in the human prefrontal cortex. Science. 302:1181–1185.

Koyama M, Hasegawa I, Osada T, Adachi Y, Nakahara K, Miyashita Y. 2004. Functional magnetic resonance imaging of macaque monkeys performing visually guided saccade tasks: comparison of cortical eye fields with humans. Neuron. 41:795–807.

Krienen FM, Yeo BTT, Buckner RL. 2014. Reconfigurable state-dependent functional coupling modes cluster around a core functional architecture. Philos Trans Roy Soc B. 369:20130526.

Krzywinski M, Schein J, Birol I, Connors J, Gascoyne R, Horsman D, Jones SJ, Marra MA. 2009. Circos: an information esthetic for comparative genomics. Genome Res. 19:1639–1645.

Laird AR, Fox PM, Eickhoff SB, Turner JA, Ray KL, McKay DR, Glahn DC, Beckmann CF, Smith SM, Fox PT. 2011. Behavioral interpretations of intrinsic connectivity networks. J Cogn Neurosci. 23:4022–4037.

Lancaster JL, Tordesillas-Gutiérrez D, Martinez M, Salinas F, Evans A, Zilles K, Mazziotta JC, Fox PT. 2007. Bias between MNI and Talairach coordinates analyzed using the ICBM-152 brain template. Hum Brain Mapp. 28:1194–1205.

Langer R, Rottschy C, Laird AR, Fox PT, Eickhoff SB. 2014. Meta-analytic connectivity modelling revisited: controlling for activation base rates. Neuroimage. 99:559–570.

Lenartowicz A, Kalar DJ, Congdon E, Poldrack RA. 2010. Towards an ontology of cognitive control. Topics Cogn Sci. 2:678–692.

Markov NT, Ercsey-Ravasz M, Van Essen DC, Knoblauch K, Toroczkai Z, Kennedy H. 2013. Cortical high-density counterstream architectures. Science. 342:1238406.

McIntosh AR. 2000. Towards a network theory of cognition. Neural Netw. 13:861–870.

Mennes M, Kelly C, Colcombe S, Castellanos FX, Milham MP. 2013. The extrinsic and intrinsic functional architectures of the human brain are not equivalent. Cereb Cortex. 23:223–229.

Menon V, Uddin LQ. 2010. Saliency, switching, attention and control: a network model of insula function. Brain Struct Funct. 214:655–667.

Mesulam M. 1990. Large-scale neurocognitive networks and distributed processing for attention, language, and memory. Ann Neurol. 28:597–613.

Mesulam MM. 1998. From sensation to cognition. Brain. 121:1013–1052.

Miller EK, Cohen JD. 2001. An integrative theory of prefrontal cortex function. Ann Rev Neurosci. 24:167–202.

Mitchell JP. 2008. Activity in right temporo-parietal junction is not selective for theory-of-mind. Cereb Cortex. 18:262–271.

Miyake A, Friedman NP, Emerson MJ, Witzki AH, Howerter A, Wager TD. 2000. The unity and diversity of executive functions and their contributions to complex "frontal lobe" tasks: a latent variable analysis. Cogn Psych. 41:49–100.

Niendam TA, Laird AR, Ray KL, Dean YM, Glahn DC, Carter CS. 2012. Meta-analytic evidence for a superordinate cognitive control network subserving diverse executive functions. Cogn Affect Behav Neurosci. 12:241–268.

Pandya DN, Kuypers HG. 1969. Cortico-cortical connections in the rhesus monkey. Brain Res. 13:13–36.

Passingham RE, Stephan KE, Kötter R. 2002. The anatomical basis of functional localization in the cortex. Nat Rev Neurosci. 3:606–616.

Petrides M. 2005. Lateral prefrontal cortex: architectonic and functional organization. Philos Trans R Soc Lond B. 360:781–795.

Poldrack RA. 2006. Can cognitive processes be inferred from neuroimaging data? Trends Cogn Sci. 10:59–63.

Poldrack RA. 2011. Inferring mental states from neuroimaging data: from reverse inference to large-scale decoding. Neuron. 72:692–697.

Poldrack RA, Mumford JA, Schonberg T, Kalar D, Barman B, Yarkoni T. 2012. Discovering relations between mind, brain, and mental disorders using topic mapping. PLoS Comp Biol. 8:e1002707.

Posner MI, Petersen SE, Fox PT, Raichle ME. 1988. Localization of cognitive operations in the human brain. Science. 240:1627–1631.

Power JD, Cohen AL, Nelson SM, Wig GS, Barnes KA, Church JA, Vogel AC, Laumann TO, Miezin FM, Schlaggar BL. 2011. Functional network organization of the human brain. Neuron. 72:665–678.

Price CJ, Friston KJ. 2005. Functional ontologies for cognition: the systematic definition of structure and function. Cogn Neuropsych. 22:262–275.

Rigotti M, Barak O, Warden MR, Wang X-J, Daw ND, Miller EK, Fusi S. 2013. The importance of mixed selectivity in complex cognitive tasks. Nature. 497:585–590.

Rosen-Zvi M, Chemudugunta C, Griffiths T, Smyth P, Steyvers M. 2010. Learning author-topic models from text corpora. ACM Trans Inform Syst. 28:1–38.

Rottschy C, Langner R, Dogan I, Reetz K, Laird AR, Schulz JB, Fox PT, Eickhoff SB. 2012. Modelling neural correlates of working memory: a coordinate-based meta-analysis. NeuroImage. 60:830–846.

Salimi-Khorshidi G, Nichols TE, Smith SM, Woolrich MW. 2011. Using gaussian-process regression for meta-analytic neuroimaging inference based on sparse observations. IEEE Trans Med Imaging. 30:1401–1416.

Saygin ZM, Osher DE, Koldewyn K, Reynolds G, Gabrieli JD, Saxe RR. 2012. Anatomical connectivity patterns predict face selectivity in the fusiform gyrus. Nat Neurosci. 15:321–327.

Shackman AJ, Salomons TV, Slagter HA, Fox AS, Winter JJ, Davidson RJ. 2011. The integration of negative affect, pain and cognitive control in the cingulate cortex. Nat Rev Neurosci. 12:154–167.

Shenhav A, Botvinick MM, Cohen JD. 2013. The expected value of control: an integrative theory of anterior cingulate cortex function. Neuron. 79:217–240.

Smith SM, Fox PT, Miller KL, Glahn DC, Fox PM, Mackay CE, Filippini N, Watkins KE, Toro R, Laird AR et al. 2009. Correspondence of the brain's functional architecture during activation and rest. Proc Natl Acad Sci USA. 106:13040–13045.

Smith SM, Jenkinson M, Woolrich MW, Beckmann CF, Behrens TEJ, Johansen-Berg H, Bannister PR, De Luca M, Drobnjak I, Flitney DE et al. 2004. Advances in functional and structural MR image analysis and implementation as FSL. NeuroImage. 23: S208–S219.

Spreng RN, Stevens WD, Chamberlain JP, Gilmore AW, Schacter DL. 2010. Default network activity, coupled with the frontoparietal control network, supports goal-directed cognition. NeuroImage. 53:303–317.

Stoodley CJ, Schmahmann JD. 2009. Functional topography in the human cerebellum: a meta-analysis of neuroimaging studies. NeuroImage. 44:489–501.

Szczepanski SM, Konen CS, Kastner S. 2010. Mechanisms of spatial attention control in frontal and parietal cortex. J Neurosci. 30:148–160.

Thompson-Schill SL, D'Esposito M, Aguirre GK, Farah MJ. 1997. Role of left inferior prefrontal cortex in retrieval of semantic knowledge: a reevaluation. Proc Natl Acad Sci USA. 94:14792–14797.

Ungerleider LG, Desimone R. 1986. Cortical connections of visual area MT in the macaque. J Comp Neurol. 248:190–222.

Van Essen DC, Dierker DL. 2007. Surface-based and probabilistic atlases of primate cerebral cortex. Neuron. 56:209–225.

Van Essen DC, Glasser MF, Dierker DL, Harwell J, Coalson T. 2012. Parcellations and hemispheric asymmetries of human cerebral cortex analyzed on surface-based atlases. Cereb Cortex. 22: 2241–2262.

Varoquaux G, Schwartz Y, Pinel P, Thirion B. 2013. Cohort-level brain mapping: learning cognitive atoms to single out specialized regions. Lect Notes Comput Sc. 7917:438–449.

Wager TD, Lindquist M, Kaplan L. 2007. Meta-analysis of functional neuroimaging data: current and future directions. Soc Cogn Affect Neurosci. 2:150–158.

Wagner AD, Paré-Blagoev EJ, Clark J, Poldrack RA. 2001. Recovering meaning: left prefrontal cortex guides controlled semantic retrieval. Neuron. 31:329–338.

Walton GL, Paul WE. 1901. Contribution to the study of the cortical sensory areas. Brain. 24:430–452.

Wise SP. 2008. Forward frontal fields: phylogeny and fundamental function. Trends Neurosci. 31:599–608.

Yarkoni T, Poldrack RA, Nichols TE, Van Essen DC, Wager TD. 2011. Large-scale automated synthesis of human functional neuroimaging data. Nat Methods. 8:665–670.

Yeo BTT, Krienen FM, Chee MWL, Buckner RL. 2014. Estimates of segregation and overlap of functional connectivity networks in the human cerebral cortex. Neuroimage. 88:212–227.

Yeo BTT, Krienen FM, Sepulcre J, Sabuncu MR, Lashkari D, Hollinshead M, Roffman JL, Smoller JW, Zöllei L, Polimeni JR et al. 2011. The organization of the human cerebral cortex estimated by intrinsic functional connectivity. J Neurophysiol. 106:1125–1165.

Yeo BTT, Sabuncu MR, Vercauteren T, Ayache N, Fischl B, Golland P. 2010. Spherical demons: fast diffeomorphic landmark-free surface registration. IEEE Trans Med Imaging. 29:650–668.

Young L, Camprodon JA, Hauser M, Pascual-Leone A, Saxe R. 2010. Disruption of the right temporoparietal junction with transcranial magnetic stimulation reduces the role of beliefs in moral judgments. Proc Natl Acad Sci USA. 107:6753–6758.

Yue YR, Lindquist MA, Loh JM. 2012. Meta-analysis of functional neuroimaging data using Bayesian nonparametric binary regression. Ann Appl Stat. 6:697–718.